



Impact de fonte tardive ou hâtive de neige et de glace sur l'export de microalgues dans la mer de Beaufort

Mémoire

Gabrielle Nadaï

Maîtrise en biologie - avec mémoire
Maître ès sciences (M. Sc.)

Québec, Canada

Impact de fonte tardive ou hâtive de neige et de glace sur l'export de microalgues dans la mer de Beaufort

Mémoire

Gabrielle Nadaï

Sous la direction de :

Louis Fortier

Et la codirection de :

Jean-Éric Tremblay

Résumé

Les observations dérivées d'images satellites suggèrent que la réduction récente de l'étendue de la glace de mer a entraîné une augmentation de la production primaire en Arctique. Cependant, peu d'observations in situ sont disponibles pour confirmer ces estimations, en particulier au début de la saison de production. Les cellules de microalgues collectées dans des pièges à particules déployés sur trois sites de la mer de Beaufort au cours de trois à cinq cycles annuels de 2011 à 2017 ont été énumérées et identifiées afin d'étudier les changements dans le timing, l'abondance et la composition de l'export de microalgues en relation avec les variations dans le couvert de neige et de glace de mer. Les diatomées ont dominé les flux de microalgues avec différents assemblages au printemps-été (avril à août; *Fragilariopsis* spp. et *Thalassiosira* spp.) et à l'automne (septembre-novembre; *Cylindrotheca closterium*). La fonte des neiges ou la débâcle des glaces s'est produite dès la fin avril (2016) et jusqu'à la mi-août (2013). Les flux printemps-été des diatomées variaient de 0,05 à 500 mg C m⁻² (< 10⁵ à 1,25 x 10¹⁰ cellules m⁻²) et étaient négativement corrélés à la date de la fonte des neiges ($r^2 = 0,35$, $n = 12$) et à la débâcle des glaces ($r^2 = 0,32$, $n = 12$). L'exportation de l'algue de glace *Nitzschia frigida* reflète la libération des algues de glace au début de la fonte des neiges. Les flux maximaux de diatomées ont été systématiquement observés peu de temps après la débâcle des glaces. La contribution en pourcentage du flux de carbone associé aux microalgues (MC) au flux de carbone organique particulaire (POC) augmente avec l'ampleur du flux de diatomées. L'ampleur du flux de diatomées automnal relativement faible n'était pas corrélée de manière significative à la date de formation du couvert de glace ($r^2 = 0,24$, $n = 10$). Nos résultats sont généralement cohérents avec les observations satellitaires suggérant une augmentation de la biomasse de microalgues et le développement d'une prolifération de diatomées à l'automne en réponse à une saison libre plus longue dans les mers arctiques. Les variations à l'échelle régionale dans le régime de neige et de glace de mer ont une incidence directe sur le moment et l'ampleur de la production de microalgues et sur sa contribution à l'export de POC dans la mer de Beaufort. Avec le réchauffement climatique, la réduction continue du couvert de neige et de glace dans les mers arctiques entraînera une augmentation des flux de carbone vers le benthos et, potentiellement, une séquestration du carbone en profondeur.

Abstract

Microalgal cells collected in sediment traps deployed at three sites in the Beaufort Sea during three to five annual cycles from 2011 to 2017 were enumerated and identified to investigate changes in the timing, abundance and composition of microalgal export in relation to variations in snow and sea ice cover. Diatoms dominated the microalgal fluxes with different assemblages in spring-summer (April to August; *Fragilariopsis* spp. and *Thalassiosira* spp.) and autumn (September-November; *Cylindrotheca closterium*). Snowmelt or ice breakup occurred as early as late April (2016) and as late as mid-August (2013). The magnitude of the spring-summer diatom flux varied from ~0.05 to 500 mg C m⁻² (< 10⁵ to 1.25 x 10¹⁰ cells m⁻²) and was negatively correlated to snowmelt date ($r^2 = 0.35$, $n = 12$) and sea-ice breakup date ($r^2 = 0.32$, $n = 12$). The export of the ice-obligated algae *Nitzschia frigida* reflected the release of sea ice algae at the onset of snowmelt. Peak diatom fluxes were consistently observed shortly after sea-ice break-up. The percent contribution of microalgal carbon to the particulate organic carbon (POC) flux increased with the magnitude of the diatom flux. The magnitude of the relatively small autumnal diatom flux was not significantly correlated to freeze-up date ($r^2 = 0.24$, $n = 10$). Our results are generally consistent with satellite observations suggesting an increase in microalgal biomass and the development of an autumn diatom bloom in response to a longer ice-free season in Arctic seas. Variations at the regional scale in the snow and sea-ice regimes directly impact the timing and magnitude of microalgal production and its contribution to POC export in the Beaufort Sea. With global warming, the ongoing reduction of the sea-ice cover in Arctic seas will result in increased carbon fluxes to the benthos and, potentially, carbon sequestration at depth.

Table des matières

Résumé	ii
Abstract.....	iii
Table des matières	iv
Liste des figures.....	v
Liste des tableaux	vi
Liste des abréviations, sigles, acronymes.....	vii
Remerciements	viii
Avant-propos	ix
Introduction	1
Production primaire en Arctique.....	1
Réchauffement climatique	2
Région d'étude.....	4
Mouillage et pièges à particules.....	5
Objectifs de l'étude.....	5
Impact of early and late snowmelt and sea ice break-up on microalgal export in the Beaufort Sea	6
1.1 Résumé.....	6
1.2 Abstract.....	7
2. Introduction.....	8
3. Material and Methods	10
3.1 Satellite-derived observations	10
3.2 Sequential sediment traps.....	10
3.3 Microalgal fluxes.....	13
3.4 Particulate organic carbon fluxes	13
4. Results.....	14
4.1 Sea ice concentration and snow depth.....	14
4.2 Microalgal fluxes.....	14
4.3 Microalgal flux composition	18
4.4 Seasonal and annual diatom and MC fluxes	21
5. Discussion	23
5.1. Impact of early snowmelt and sea ice break-up	23
5.2. Impact of late snowmelt and sea ice break-up	29
5.3. Impact of a late sea ice freeze-up.....	30
5.4. Influence of the Mackenzie River	31
6. Conclusion	31
7. Acknowledgments	32
8. Funding	32
Conclusion générale	33
Bibliographie	36

Liste des figures

Figure 1: Saisonnalité du développement de la floraison printanière en Arctique. Tiré de Wassman et al. 2011.....	1
Figure 2: Schéma d'un mouillage (gauche) et d'un piège à particule (droite).....	5
Figure 3: Position des trois sites de mouillage.....	6
Figure 4: Positions of the three mooring sites in the Beaufort Sea. Colored lines represent the annual September sea ice minimum extent from 2012 to 2017.....	12
Figure 5: Daily snow depth (gray) and sea ice concentration (black) over the three mooring sites.	17
Figure 6: Microalgal fluxes at the three mooring sites. Panels with grey backgrounds show deployment under 300 m. Note the different scales.....	18
Figure 7: Fluxes of the 15 most abundant diatom groups at the three mooring sites. Panels with grey backgrounds show deployment under 300 m. Note the different scales.	20
Figure 8: Fluxes of the ice-obligated diatom <i>Nitzschia frigida</i> and the freshwater diatom group <i>Diatoma/Asterionella</i> spp. at the three mooring sites. Panels with grey backgrounds show deployments under 300 m.	21
Figure 9: Absolute (a) and relative (b) microalgal fluxes and absolute (c) and relative (d) microalgal carbon fluxes for autumn (September to November) and spring/summer (April to August) for the 15 most abundant diatoms groups collected at the three mooring sites.	23
Figure 10: Correlation between (a) the onset of snowmelt (M) and the dates of maximum diatom flux (DFD) using the first day of collection period, and (b) the date of sea ice break-up (B) and the dates of maximum diatom flux using the first day of collection period.	27
Figure 11: Correlation between (a) the onset of snowmelt (M) and the spring/summer diatom fluxes (DF), (b) the date of sea ice break-up (B) and the spring/summer diatom fluxes, (c) the onset of snowmelt and the spring/summer MC fluxes (MCF), and (d) the date of sea ice break-up and the spring/summer MC fluxes. Regression equations are given with the p value of the slope and marginal r^2	28

Liste des tableaux

Table 1. Mooring and sediment trap deployment information. Number in parentheses are julian days.....	13
Table 2. Annual microalgal (MC) and contributions of MC to the POC fluxes (in parentheses, in %) at the three sites.....	22

Liste des abréviations, sigles, acronymes

POC : particulate organic carbon/carbone organique particulaire

MC : Microalgal carbon/ carbone microalgal

Remerciements

Je souhaite remercier les organismes subventionnaires : le Conseil de recherches en sciences naturelles et en génie du Canada et le Fonds québécois de la recherche sur la nature et les technologies pour les bourses ayant financé ma maîtrise, ainsi que Québec-Océan, ArcticNet et Sentinelle Nord, pour le soutien financier m'ayant permis d'assister à plusieurs conférences et de suivre un cours à Svalbard.

Ce projet a bénéficié de l'aide précieuse de plusieurs personnes. Merci à mon directeur, Louis Fortier, de m'avoir donné la chance d'entrer dans le monde de la recherche. Merci à Catherine Lalande, qui a endossé le rôle de co-superviseure, mentor et amie.

Merci à l'équipe du Labo Fortier. Je voudrais spécialement remercier Marie Parenteau, qui a effectué les analyses taxonomiques des microalgues pour mon projet. Merci à Thibaud Dezutter pour les données de concentration de glace et de couvert de neige. Merci à Cyril Aubry, Sarah Schembri, Gérald Darnis, Rosalee Strassburg-Huot et Tommy Pontbriand pour leur aide en laboratoire et leur soutien. Un grand merci à Mathieu LeBlanc, mon colocataire de bureau et équipier sur l'*Amundsen*, pour son mentorat qui a souvent calmé mes inquiétudes.

Merci à l'équipage du NGCC *Amundsen* et aux techniciens d'ArcticNet, pour le déploiement et la récupération des mouillages.

Finalement, un merci tout spécial à ma famille et à mon amoureux. Merci de vous intéresser à ce que je fais, même si vous ne comprenez pas pourquoi je suis obsédée par l'export de carbone. Merci d'avoir tout fait pour faciliter mes études.

Avant-propos

Le corps de ce mémoire a été rédigé en anglais sous forme d'article scientifique, dont je serai l'auteure principale, pour fin de publication dans le *Journal of Plankton Research*. J'ai effectué les analyses de carbone organique particulaire des pièges à particules. Marie Parenteau a effectué les analyses taxonomiques des microalgues. Thibaud Dezutter a fourni les données de concentration de glace et d'épaisseur du couvert de neige. J'ai traité toutes les données qui ont été obtenues et calculé le carbone microalgal à partir des biovolumes mesurés par Eva-Maria Nöthig de l'Alfred-Wegener Institute Helmholtz Centre for Polar and Marine Research en Allemagne. J'ai rédigé l'ensemble du manuscrit sous la supervision de Catherine Lalande et de Louis Fortier, d'où leur statut de coauteur de cet article.

Introduction

Production primaire en Arctique

L'océan Arctique est caractérisé par une saisonnalité extrême dans son régime lumineux et son régime de glace et de neige. De la nuit polaire au soleil de minuit, la présence ou l'absence de glace de mer et de neige régissent la production de microalgues tant à l'intérieur de la glace que dans la colonne d'eau (Fig. 1).

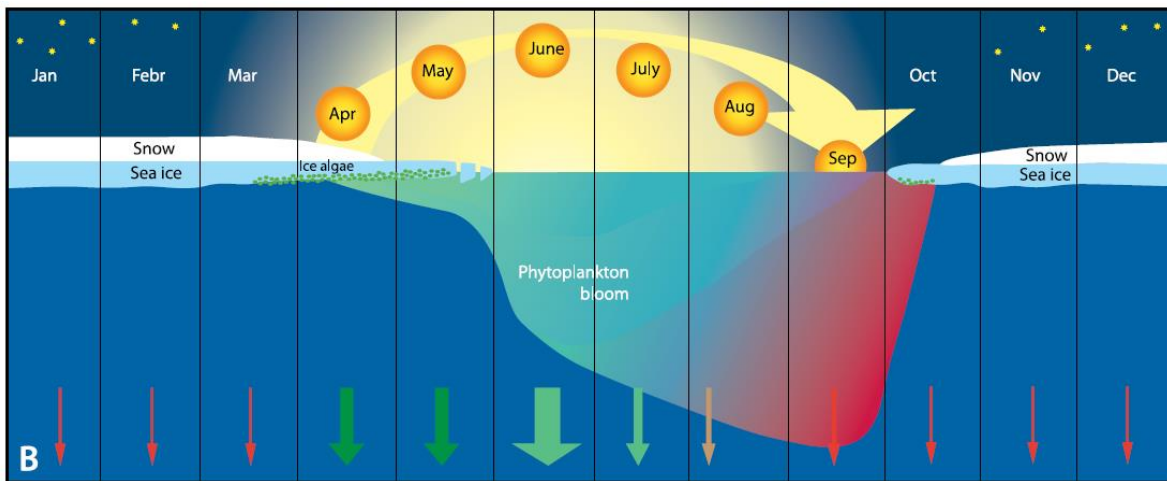


Figure 1: Saisonnalité du développement de la floraison printanière en Arctique. Tiré de Wassman et al. 2011.

Un couvert de glace saisonnier, dont l'étendue maximale est atteinte en mars et l'étendue minimale en septembre, perdure dans l'Océan Arctique durant près de 9 mois, ce qui restreint la production primaire à une courte période (Horner and Schrader, 1982; Stern and Gaden, 2015). La croissance du phytoplancton, des organismes photosynthétiques unicellulaires allant du picoplancton ($<2 \mu\text{m}$) au mégaplancton ($>2000 \mu\text{m}$), est d'abord limitée par la lumière et ensuite par la disponibilité des nutriments, plus spécifiquement par le nitrate (Tremblay et al., 2008; Tremblay and Gagnon, 2009). La glace de mer se forme rapidement au début de la nuit polaire, ce qui conduit en automne à l'incorporation dans la glace de cellules de microalgues en suspension (Horner and Schrader, 1982; Syvertsen, 1991). La biomasse d'algues de glace de mer, majoritairement des espèces de diatomées pennées colonisant la couche inférieure de la glace, reste faible pendant la nuit polaire et augmente avec l'augmentation progressive de la lumière au printemps, même sous une épaisse couche de neige et de glace de mer (Horner and Schrader, 1982; Juul-Pedersen et al., 2008). En fonction des régions, les algues de glace peuvent représenter entre 2 et 58 % de la

production primaire totale (Gosselin et al., 1997), et peuvent même surpasser la production primaire pélagique au début du printemps sur le plateau de la mer de Chukchi (Gradinger, 2009). La biomasse d'algues de glace continue d'augmenter jusqu'à ce que les conditions se dégradent et entraînent leur libération dans la colonne d'eau, probablement à cause d'un réchauffement et d'une ablation de la glace de mer et d'une exposition à des niveaux élevés d'irradiance après la fonte du couvert de neige ainsi qu'au choc osmotique causé par l'eau de fonte (Fortier et al., 2002; Campbell et al., 2015). Les algues de glace représentent une première source de carbone pour le réseau trophique sympagique, vivant en association étroite avec la glace, et pélagique (Budge et al., 2008; Kohlbach et al., 2016). Une fois libérées, les algues de glace de mer peuvent être rapidement exportées vers le fond marin (Michel et al., 1993), comme en témoigne la présence de tapis d'algues de glace au fond de l'Arctique central (Boetius et al., 2013), ou peuvent ensemençer la floraison de phytoplancton pélagique, comme en témoigne le fort chevauchement entre les espèces d'algues de glace et de phytoplancton (Syvertsen, 1991; Von Quillfeldt, 2004; Szymanski and Gradinger, 2016). À mesure que la neige et la glace fondent davantage au printemps et en été, la disponibilité accrue de la lumière et le renforcement de la stratification permettent le développement d'une floraison de phytoplancton pélagique, sous la glace ou à la marge de la glace (Fig. 1) (Fortier et al., 2002; Sakshaug, 2004; Tremblay et al., 2008; Arrigo et al., 2012; Assmy et al., 2017). Les diatomées sont majoritairement responsables de ces floraisons annuelles. Les cellules de microalgues produites lors de la fonte des glaces et en l'absence de banquise sont soit broutées par le zooplancton, alimentant le réseau trophique pélagique (Juil-Pedersen et al., 2008a; Darnis et al., 2012), soit exportées vers le fond de la mer, alimentant les communautés benthiques (Wassmann, 1997; Renaud et al., 2007). Comme la production de microalgues dépend également de la disponibilité des nutriments (Tremblay and Gagnon, 2009), la stratification en été empêche le réapprovisionnement en nutriments une fois ceux-ci consommés par les microalgues, poussant ainsi la production plus profondément dans la colonne d'eau jusqu'à une profondeur où la faible irradiance et la faible disponibilité en nutriments empêchent la croissance des microalgues (Tremblay et al., 2008). L'action du vent peut entraîner des événements de mélange et d'upwelling dans la colonne d'eau, entraînant un apport de nutriments à la surface, ce qui permet d'alimenter la production primaire dans des conditions libres de glace (Tremblay et al., 2008; Tremblay et al., 2011). Les vents favorables à la création d'upwelling étant généralement les plus forts à l'automne (Yang, 2009), une deuxième floraison de

phytoplancton peut avoir lieu avant que la couverture de glace de mer ne se forme (Ardyna et al., 2014).

Réchauffement climatique

L'Arctique est la région où la hausse des températures en réponse au réchauffement climatique est la plus marquée (Liu et al., 2007; IPCC, 2014). Les observations satellitaires démontrent que l'étendue minimale du couvert de glace de mer en été est en diminution accélérée depuis les 15 dernières années (Serreze et al., 2003; Arrigo et al., 2008; Arrigo et al., 2012). Certains modèles prévoient d'ailleurs un été libre de glace d'ici 2050 (Holland et al., 2006; Stroeve et al., 2012; Wang and Overland, 2012). De 1998 à 2012, les images satellites ont révélé une augmentation de la production primaire nette de 5 à 10 % sur la majorité des plateaux continentaux en réponse à la prolongation de la période d'eau ouverte et de croissance du phytoplancton (Arrigo and van Dijken, 2015). La tendance à long terme est cependant difficile à prédire, puisque les prévisions des modèles varient en fonction des régions étudiées et des modèles utilisés (Lavoie et al., 2010; Vancoppenolle et al., 2013).

Le réchauffement climatique est susceptible de modifier la floraison printanière en transformant les variables influençant la stratification, à savoir le couvert de glace, la température de l'eau et la salinité de la couche de surface. Dans un contexte de hausse des températures, les apports d'eau douce par les fleuves sont plus importants et se font plus tôt, ce qui renforce la stratification (ACIA, 2004). Ce phénomène est accentué par l'augmentation des précipitations au-dessus de l'océan Arctique (Christensen and Christensen, 2003). Le renforcement de la stratification dans le bassin du Canada entre 2004 et 2008 a favorisé les plus petites espèces de phytoplancton en raison de leur plus grande efficacité à assimiler des nutriments (Li et al., 2009). Les petites espèces de microalgues doivent être exportées verticalement par un processus physique entraînant l'enfoncement de masse d'eau de surface (Wollenburg et al., 2018; Lalande et al., 2019), contrairement aux diatomées qui coulent rapidement grâce à leur frustule de silice (Turner, 2002), et leur augmentation au détriment des diatomées pourrait changer l'export vertical de carbone dans l'écosystème. Le réchauffement climatique influence également l'écosystème en modifiant la force et la trajectoire des tempêtes (ACIA, 2004; Simmonds and Keay, 2009). Des tempêtes plus fortes et plus fréquentes favorisent le brassage de la colonne d'eau et mènent à un apport

de nutriments en surface (Stabeno et al., 2001). Une formation tardive du couvert de glace en automne prolonge l'exposition de la surface de l'océan à l'action du vent. Cet apport de nutriments supplémentaire permet une seconde floraison de phytoplancton à l'automne. En effet, la fréquence des floraisons automnales a augmenté de 8 à 70 % en fonction des régions dans l'océan Arctique entre les périodes de 1998-2001 et 2007-2012 (Ardyna et al., 2014).

Région d'étude

La mer de Beaufort est située au nord du Yukon et des Territoires du Nord-Ouest. Trois masses d'eau y prévalent: la couche polaire mélangée en surface (0 - 50 m), la couche pacifique intermédiaire (50 – 200 m) et la couche atlantique profonde (> 200 m) (Carmack et al., 1989). De façon générale, le déplacement des masses d'eau dans la région d'étude se fait en suivant la côte, en provenance du détroit de Béring vers le golfe d'Amundsen. Le plateau du Mackenzie reçoit également les apports d'eau douce en provenance du fleuve Mackenzie, un des fleuves avec le débit le plus important de l'océan arctique (Williams and Carmack, 2015; Pauly, 2016). Normalement, l'eau douce qui se déverse du fleuve Mackenzie s'écoule en direction est le long de la péninsule de Tuktoyaktuk vers le golfe d'Amundsen sous l'effet de la force de Coriolis (Carmack and Macdonald, 2002).

Dans la mer de Beaufort, le couvert de glace de mer a complètement fondu en septembre 2012 pour la première fois depuis le début de l'étude de cette région par imagerie satellite (Babb et al., 2016). Les observations dérivées d'images satellites ont également indiqué que, bien que le moment de la débâcle de la glace de mer dans la mer de Beaufort soit resté inchangé de 1983 à 2014, la formation du couvert de glace de mer était retardée chaque année, prolongeant la période libre de glace (Galley et al., 2016). Une période d'eau libre et une saison de croissance du phytoplancton plus longue pourraient potentiellement augmenter la production primaire annuelle, comme cela a déjà été observé pour plusieurs régions de l'océan Arctique, selon les concentrations de chlorophylle *a* (chl *a*) de surface obtenues par satellite (Arrigo et al., 2012). Le retrait plus prononcé de la marge de glace au nord du talus continental de la mer de Beaufort, associé à la diminution de l'étendue du couvert de glace, facilite également les upwellings en provoquant la remontée d'eau profonde riche en nutriments le long du talus suite à l'action du vent (Carmack and Chapman, 2003; Mundy et al., 2009). De plus, une formation du couvert de glace de mer de plus en plus tardive dans la

aux variations interannuelles dans la date de fonte du couvert de neige et de débâcle de la banquise au printemps; et (2) de déterminer l'impact d'une formation tardive du couvert de glace sur les flux de microalgues et de MC en automne.

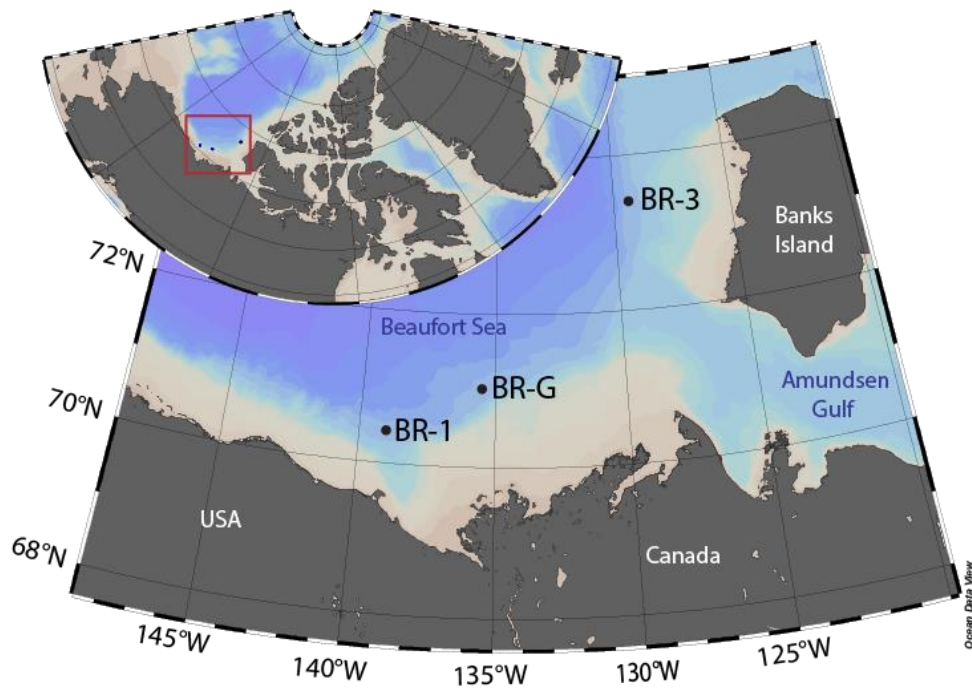


Figure 3: Position des trois sites de mouillage

Early snowmelt and sea ice breakup magnify export to depth in the Beaufort Sea

1.1 Résumé

Les cellules de microalgues collectées dans des pièges à particules déployés sur trois sites de la mer de Beaufort au cours de trois à cinq cycles annuels de 2011 à 2017 ont été énumérées et identifiées afin d'étudier les changements dans le timing, l'abondance et la composition de l'export de microalgues en relation avec les variations dans le couvert de neige et de glace de mer. Les diatomées ont dominé les flux de microalgues avec différents assemblages au printemps-été (avril à août; *Fragilariopsis* spp. et *Thalassiosira* spp.) et à l'automne (septembre-novembre; *Cylindrotheca closterium*). La fonte des neiges ou la débâcle des glaces s'est produite dès la fin avril (2016) et jusqu'à la mi-août (2013). Les flux printemps-été des diatomées variaient de 0,05 à 500 mg C m⁻² (< 10⁵ à 1,25 x 10¹⁰ cellules m⁻²) et étaient négativement corrélés à la date de la fonte des neiges ($r^2 = 0,35$, n = 12) et à la débâcle des glaces ($r^2 = 0,32$, n = 12). L'exportation de l'algue de glace *Nitzschia frigida* reflète la libération des algues de glace au début de la fonte des neiges. Les flux maximaux de diatomées ont été systématiquement observés peu de temps après la débâcle des glaces. La contribution en pourcentage du flux de carbone associé aux microalgues (MC) au flux de carbone organique particulaire (POC) augmente avec l'ampleur du flux de diatomées. L'ampleur du flux de diatomées automnal relativement faible n'était pas corrélée de manière significative à la date de formation du couvert de glace ($r^2 = 0,24$, n = 10). Nos résultats sont généralement cohérents avec les observations satellitaires suggérant une augmentation de la biomasse de microalgues et le développement d'une prolifération de diatomées à l'automne en réponse à une saison libre plus longue dans les mers arctiques. Les variations à l'échelle régionale dans le régime de neige et de glace de mer ont une incidence directe sur le moment et l'ampleur de la production de microalgues et sur sa contribution à l'export de POC dans la mer de Beaufort. Avec le réchauffement climatique, la réduction continue du couvert de neige et de glace dans les mers arctiques entraînera une augmentation des flux de carbone vers le benthos et, potentiellement, une séquestration du carbone en profondeur.

1.2 Abstract

Microalgal cells collected in sediment traps deployed at three sites in the Beaufort Sea during three to five annual cycles from 2011 to 2017 were enumerated and identified to investigate changes in the timing, abundance and composition of microalgal export in relation to variations in snow and sea ice cover. Diatoms dominated the microalgal fluxes with different assemblages in spring-summer (April to August; *Fragilariopsis* spp. and *Thalassiosira* spp.) and autumn (September-November; *Cylindrotheca closterium*). Snowmelt or ice breakup occurred as early as late April (2016) and as late as mid-August (2013). The magnitude of the spring-summer diatom flux varied from ~0.05 to 500 mg C m⁻² (< 10⁵ to 1.25 x 10¹⁰ cells m⁻²) and was negatively correlated to snowmelt date ($r^2 = 0.35$, $n = 12$) and sea-ice breakup date ($r^2 = 0.32$, $n = 12$). The export of the ice-obligated algae *Nitzschia frigida* reflected the release of sea ice algae at the onset of snowmelt. Peak diatom fluxes were consistently observed shortly after sea-ice break-up. The percent contribution of microalgal carbon to the particulate organic carbon (POC) flux increased with the magnitude of the diatom flux. The magnitude of the relatively small autumnal diatom flux was not significantly correlated to freeze-up date ($r^2 = 0.24$, $n = 10$). Our results are generally consistent with satellite observations suggesting an increase in microalgal biomass and the development of an autumn diatom bloom in response to a longer ice-free season in Arctic seas. Variations at the regional scale in the snow and sea-ice regimes directly impact the timing and magnitude of microalgal production and its contribution to POC export in the Beaufort Sea. With global warming, the ongoing reduction of the sea-ice cover in Arctic seas will result in increased carbon fluxes to the benthos and, potentially, carbon sequestration at depth.

2. Introduction

Extreme seasonal variability in sunlight, snow cover, and sea ice cover affects most processes in the pelagic ecosystems of the Arctic Ocean. From polar night to midnight sun, the presence or absence of sea ice and snow dictates microalgal production both within the sea ice and in the photic zone of the water column. Sea ice rapidly forms at the onset of the polar night, leading to the incorporation of suspended microalgal cells into the bottom layer in autumn (Homer and Schrader, 1982; Syvertsen, 1991). The biomass of sea ice microalgae remains low during the polar night and starts to increase with increasing daylight in spring, even under thick snow and sea ice cover (Horner and Schrader, 1982; Juul-Pedersen et al., 2008). The biomass of sea ice microalgae increases until deteriorating conditions cause their release in the water column, through a combination of bottom ice warming and ablation, exposure to high levels of irradiance following snowmelt (Fortier et al., 2002; Campbell et al., 2015) and perhaps the osmotic shock caused by meltwater percolating through the sea ice. Sea ice algae provide a carbon source for the sympagic and pelagic food web, early during the season of arctic biological production (Budge et al., 2008; Kohlbach et al., 2016). Once released, sea ice algae may be rapidly exported toward the seafloor (Michel et al., 1993), as evidenced by the widespread mats of sea ice algae deposited on the deep seafloor of the central Arctic basins (Boetius et al., 2013), or may seed the pelagic bloom, as reflected by the strong overlap in sea ice and pelagic microalgal species (Syvertsen, 1991; Von Quillfeldt, 2004; Szymanski and Gradinger, 2016).

As snow and ice cover further melt during spring and summer, increased light availability and upper water stratification allow the development of a phytoplankton bloom, under the ice or at the receding ice edge (Fortier et al., 2002; Stein et al., 2004; Tremblay et al., 2008; Arrigo et al., 2012; Assmy et al., 2017). Microalgal cells produced during and after melt are either grazed by zooplankton, fueling the pelagic food web (Wassmann, 1997; Juul-Pedersen et al., 2008a) or exported toward the seafloor, feeding benthic communities (Wassmann, 1997; Renaud et al., 2007). As microalgal production also depends on nutrient availability (Tremblay and Gagnon, 2009), strong stratification preventing the replenishment of nutrients in surface waters during summer eventually limits microalgal production (Tremblay et al., 2008). Wind stress may lead to water column mixing and/or upwelling events resulting in an input of nutrients to the surface, fueling primary production under ice-free conditions

(Tremblay et al., 2008; Tremblay et al., 2011). Upwelling favorable winds are usually strongest during autumn (Yang, 2009) and autumnal blooms may take place before sea ice cover formation in the Arctic Ocean (Ardyna et al., 2014).

Earlier sea ice melt and longer open water periods have recently been observed in several regions of the Arctic Ocean (IPCC, 2014; Stroeve et al., 2014). In the Beaufort Sea in September 2012, sea ice cover melted completely for the first time since the beginning of the satellite record in 1979 (Babb et al., 2016). Remote sensing-derived observations further indicated that the annual open water duration was increasing from 1983 to 2014 (Galley et al., 2016). Longer open water periods and phytoplankton growing seasons have the potential to increase the annual marine primary production, as already reported for several regions of the Arctic Ocean based on satellite-derived surface chlorophyll *a* (chl *a*) concentrations (Arrigo and van Dijken, 2015). In addition, an increasingly late sea ice formation in the Beaufort Sea increased the probability of occurrence of autumn blooms in the region (Ardyna et al., 2014; Galley et al., 2016).

Due to difficult access by ship, most *in situ* observations in the Arctic Ocean takes place during the open water period or during advanced stages of sea ice melt, therefore after the onset of the spring bloom. Moreover, while satellites provide observations on large spatial and temporal scales, they are unable to detect chl *a* under snow and ice cover, cloud cover or at depths deeper than a few meters in the water column (Arrigo and van Dijken, 2015). These limitations result in a lack of information on the magnitude, composition, and duration of microalgal production in the Arctic Ocean, especially during spring.

Sequential sediment traps were deployed over three to five annual cycles between September 2011 and September 2017 at three sites on the Beaufort Sea shelf break to monitor seasonal and interannual variations in the timing, magnitude, and composition of microalgal fluxes in relation to snow melt and sea-ice breakup in spring and sea-ice freeze-up in autumn. Sinking ice microalgae and phytoplankton were identified to the lowest taxonomic level and the carbon fluxes associated with different species or groups were estimated.

3. Material and Methods

3.1 Satellite-derived observations

Daily averaged sea ice concentrations were retrieved at a 12.5-km resolution from the CERSAT service of the French Research Institute for Exploitation of the Sea for each mooring deployment period. Daily snow depth on top of sea ice was retrieved at a 25-km resolution from the Scanning Multichannel Microwave Radiometer (SMMR) and the Special Sensor Microwave/Imager (SSM/I) of the US National Aeronautics Space Agency for each mooring deployment period. Flagged snow depth data, data where snow depth was replaced by code assigned with specific events, were removed. Daily sea ice concentration and snow depth were averaged for a delimited region ($0.5^\circ \times 0.5^\circ$) above each mooring site.

3.2 Sequential sediment traps

Sequential sediment traps (Technicap PPS 3/3; 0.125 m² aperture, except BR-G 2011-2012: Technicap PPS 6/2; 0.5 m² aperture) were deployed at three mooring sites over the Beaufort Sea Shelf slope in the Beaufort Sea during three (BR-3), four (BR-1) or five (BR-G) annual cycles between September 2011 and September 2017 (Fig. 4; Table 1). All mooring sites were located at similar depths along the shelf break (Table 1). Moorings were deployed and recovered during the annual ArcticNet expedition on board the CCGS *Amundsen*, except in 2013 when moorings were recovered on board the CCGS *Sir Wilfrid Laurier* and not redeployed due to the late cancellation of the annual *Amundsen's* expedition. Sample collection periods were preset at intervals ranging from 8 to 31 days. Sediment trap sample cups were filled with filtered seawater poisoned with formalin (5% v/v) buffered with sodium borate and adjusted to 38 PSU with NaCl to avoid diffusion of content in ambient seawater and preserve samples during deployment and after recovery. The variation in deployment depths and the different sediment trap models potentially introduced bias when comparing the magnitude and composition of microalgal fluxes, but not their timing.

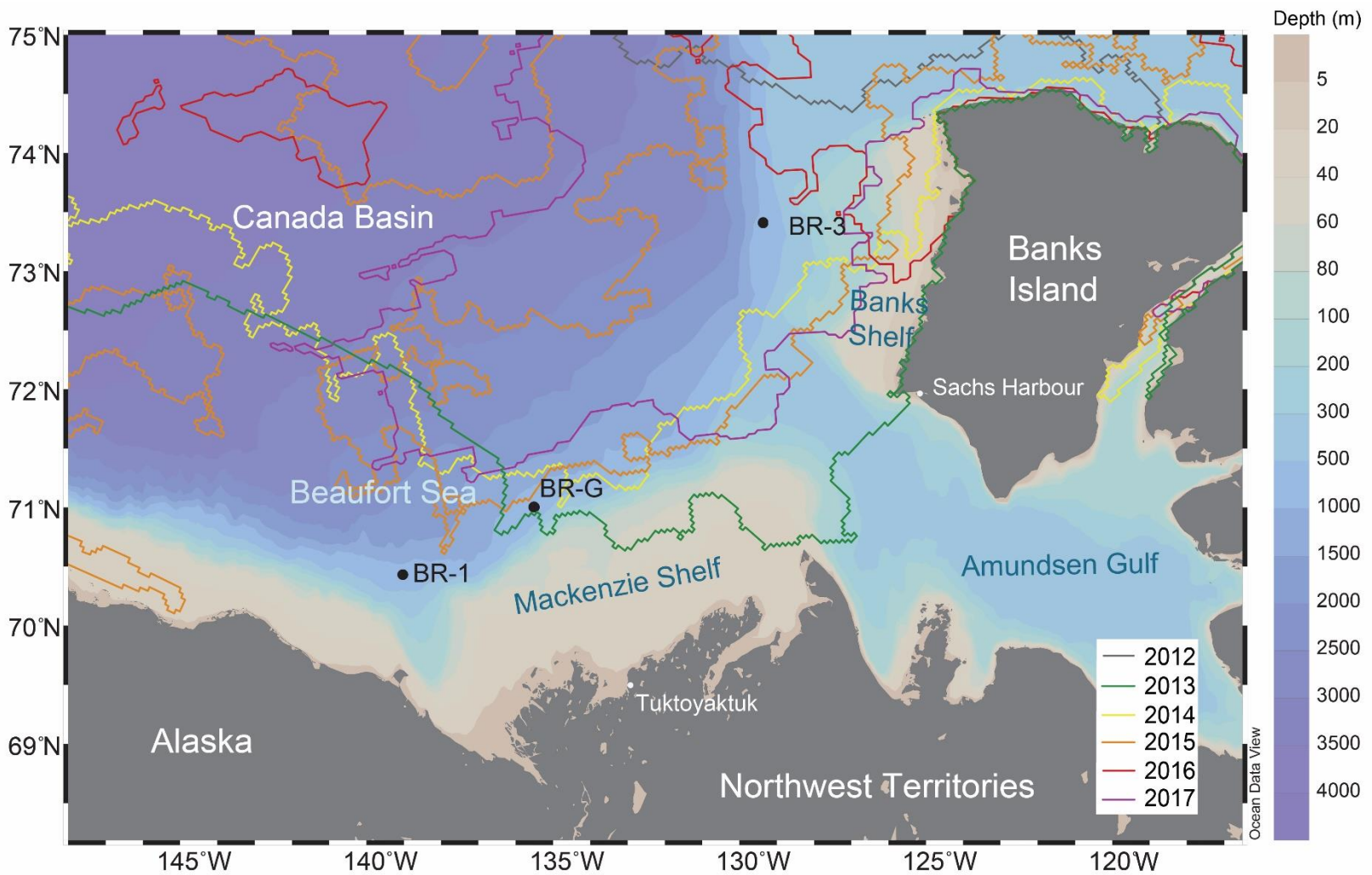


Figure 4: Positions of the three mooring sites in the Beaufort Sea. Colored lines represent the annual September sea ice minimum extent from 2012 to 2017.

Table 1: Mooring and sediment trap deployment information. Number in parentheses are Julian days.

Site	Sampling period	Latitude (°N)	Longitude (°W)	Trap depth (m)	Water depth (m)	Date sea ice freeze-up	Date snowmelt	Date sea ice break-up
BR-3	01/09/2014 - 31/08/2015	73.4086	-129.357	325	702	-	June 27 (178)	Aug 17 (229)
	04/09/2015 - 02/10/2016	73.4094	-129.354	100	690	Oct 04 (277)	July 04 (186)	Aug 03 (216)
	10/09/2016 - 01/09/2017	73.4088	-129.363	336	714	Oct 13 (287)	May 17 (137)	May 30 (150)
BR-G	20/09/2011 - 01/09/2012	71.0067	-135.500	125	705	Oct 29 (302)	May 31 (151)	May 27 (148)
	01/10/2012 - 01/10/2013	71.0078	-135.499	125	753	Nov 11 (316)	June 05 (156)	Aug 03 (215)
	01/09/2014 - 26/08/2015	71.0021	-135.509	125	702	Nov 01 (305)	May 09 (129)	May 24 (144)
	01/09/2015 - 01/09/2016	71.0020	-135.494	101	700	Oct 22 (295)	Apr 29 (120)	Apr 29 (120)
	05/09/2016 - 01/09/2017	71.0019	-135.491	299	699	Oct 30 (304)	June 07 (158)	June 01 (152)
BR-1	06/10/2012 - 01/10/2013	70.4335	-139.023	125	660	Nov 10 (315)	June 10 (161)	July 05 (186)
	03/09/2014 - 01/09/2015	70.4318	-139.023	99	754	Oct 31 (304)	May 20 (140)	May 26 (146)
	01/10/2015 - 02/10/2016	70.4318	-139.023	306	757	Oct 22 (295)	Apr 28 (119)	Apr 27 (118)
	04/09/2016 - 01/09/2017	70.4336	-139.027	120	754	Nov 05 (310)	Jun 12 (163)	June 11 (162)

3.3 Microalgal fluxes

In the laboratory, sediment trap sample cups were gently shaken to bring microalgal cells in suspension into a homogenous solution before a subsample was taken with a micropipette modified to collect large particles and placed in an Utermöhl chamber, where the final volume was adjusted to 3 ml with filtered seawater. Except for winter samples when less than 300 cells were present in the chamber, a minimum of 300 microalgal cells were enumerated and identified to the lowest taxonomic level possible by inverted microscopy at 100X, 200X or 400X magnification depending on cell size (Utermöhl, 1958). Empty microalgal cells (without chloroplasts) were distinguished from intact cells (with chloroplasts) and resting spores. Flagellates were counted but not identified. Microalgal carbon values were calculated from the estimated biovolumes of ~20 representative intact cells and resting spores for each species or group and the carbon content specific to each species or group (Edler, 1979). Daily microalgal fluxes ($\text{m}^{-2} \text{d}^{-1}$) were calculated accounting for subsample volume, trap area, and sampling period. Microalgal fluxes were integrated annually and for the spring-summer (April to August) and autumn (September to November) periods allowing a distinction between production from different year.

3.4 Particulate organic carbon fluxes

Once swimmers (zooplankton actively entering the sediment trap cups) were removed from the samples using forceps, triplicate subsamples were filtered onto Whatman GF/F filters (pore size: $0.7 \mu\text{m}$) pre-combusted at 450°C for 24 h. Filters were rinsed with distilled water to remove salt, dried for 12 h at 60°C , exposed to HCl fumes in a desiccator for 12 h to remove inorganic carbon, and dried for another 12 h before particulate organic carbon (POC) values were measured using a Perkin Elmer CHNS 2400 Series II elemental analyzer and averaged for each sample. Daily POC fluxes ($\text{m}^{-2} \text{d}^{-1}$) were calculated taking into account subsample volume, trap area, and sampling period.

4. Results

4.1 Sea ice concentration and snow depth

Sea ice freeze-up, here defined as ice concentration $>50\%$, occurred in late October or early November above the two southernmost mooring sites (BR-G and BR-1; Fig. 5; Table 1). Sea ice break-up, defined as $<50\%$ ice concentration, occurred nearly simultaneously between late April and late June at these two sites, except in 2013 when sea ice break-up occurred in early July at BR-1 and in early August at BR-G. Multiple increases in sea ice concentration were observed following the initial sea ice break-up at both sites in 2013, 2015 and 2016. The onset of snowmelt, defined as snow depth <10 cm, occurred 1 to 11 days earlier at BR-G than at BR-1 (Fig. 5; Table 1). The earliest snowmelt was recorded in late April 2016 at both BR-1 and BR-G, while the latest snowmelt was recorded in June 2013 at BR-1. Snowmelt occurred simultaneously with sea ice break-up at both sites in 2012, 2016 and 2017. The longest period between snowmelt and sea ice break-up was observed in 2013 at both sites, corresponding to four weeks at BR-1 and eight weeks at BR-G.

At the northernmost site (BR-3), sea ice concentration was $>50\%$ at the time of the mooring deployment in September 2014 (Fig. 5). Sea ice melt was incomplete during summer 2015, with sea ice concentrations remaining $>30\%$. In 2016, sea ice break-up occurred in early August, more than three months after sea ice break-up at BR-1 and BR-G. An abrupt decrease in sea ice concentration in late May 2017 was followed by a rapid increase ~ 3 weeks later. The onset of snowmelt was recorded mid-May in 2017, at the end of June in 2015 and at the beginning of July in 2016 (Fig. 5; Table 1).

4.2 Microalgal fluxes

Diatoms consistently dominated microalgal fluxes (Fig. 6). The contribution of flagellates, silicoflagellates, and coccolithophores was apparent only at times of very low diatom fluxes. A large proportion of diatoms was exported as resting spores at the northernmost site during summer and autumn 2016. Maximum diatom fluxes (including spores) ranged from ~ 0.5 million cells $\text{m}^{-2} \text{d}^{-1}$ at BR-3 in late July 2015 to ~ 300 million cells $\text{m}^{-2} \text{d}^{-1}$ at BR-G and BR-1 in late May and early June 2016, respectively. Maximums in diatom fluxes occurred at similar times between late May and early July at the two southernmost locations, except in 2017 when the maximum diatom flux occurred at the beginning of August at BR-1, one

month later than at BR-G (Fig. 6). Two maximums in microalgal fluxes were recorded at BR-1 in 2013; empty diatoms dominated the first maximum in late June while intact diatoms dominated the second maximum in early September. Relatively high fluxes of mostly empty diatoms were recorded at BR-G and BR-1 from October to late November-December 2012 and from January to late May 2017. At the northernmost site, maximums in diatom fluxes occurred in late July 2015 and in August 2016, more than six weeks later than the highest diatom fluxes recorded at the two southernmost sites. Diatom fluxes were very low at BR-3 in spring and summer 2017 (Fig. 6).

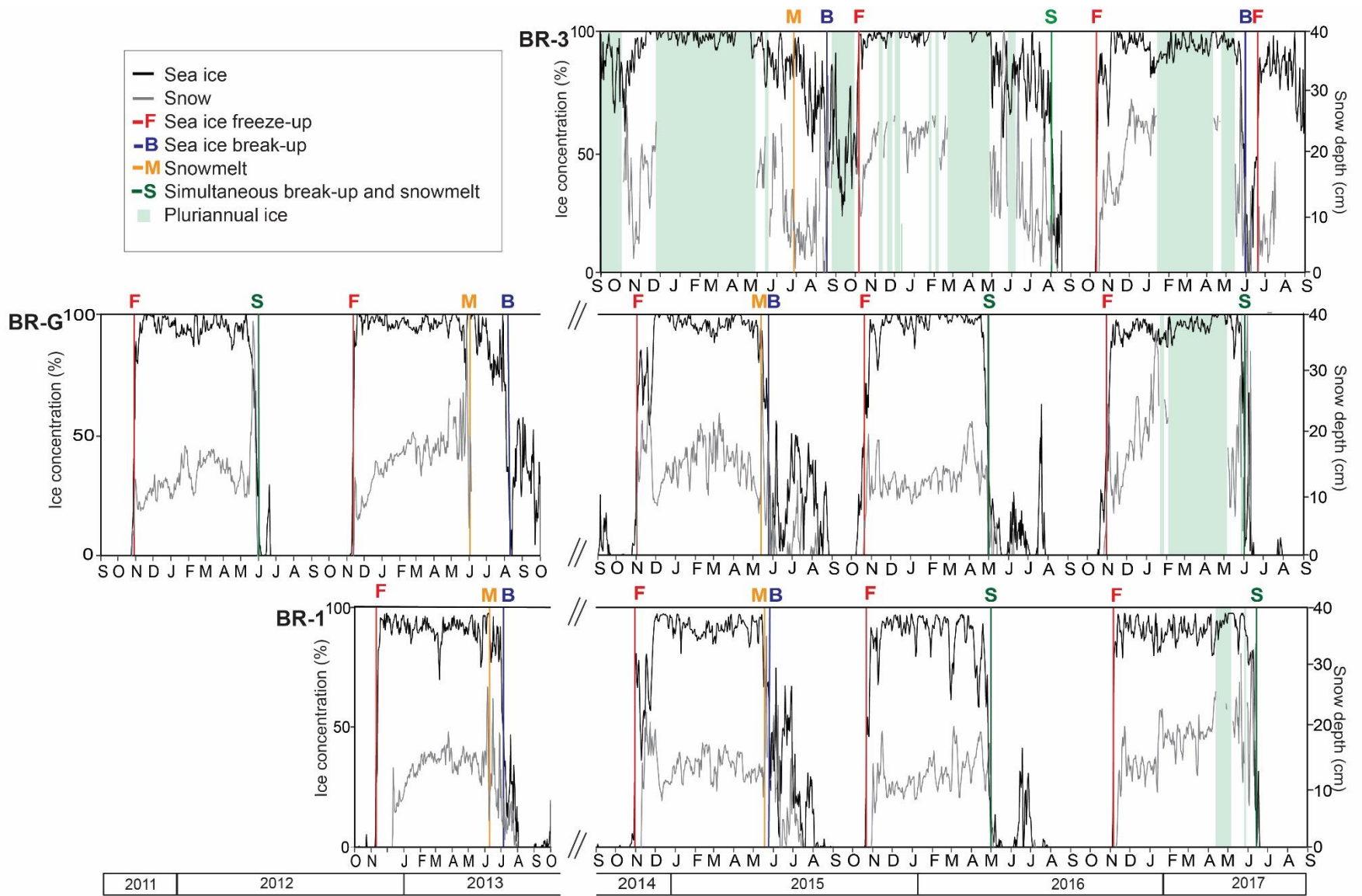


Figure 5: Daily snow depth (gray) and sea ice concentration (black) over the three mooring sites.

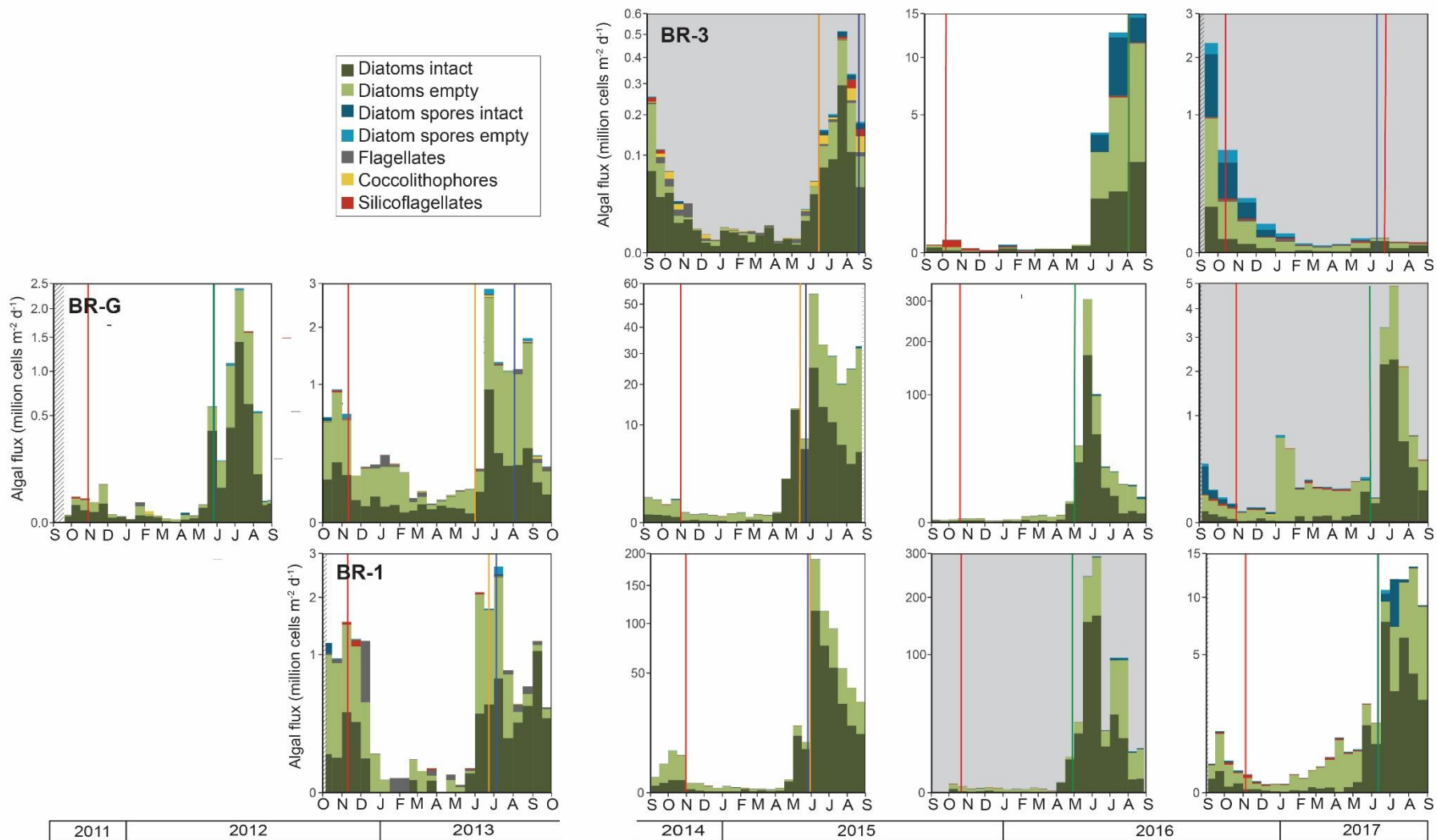


Figure 6: Microalgal fluxes at the three mooring sites. Panels with grey backgrounds show deployment under 300 m. Note the different scales.

4.3 Microalgal flux composition

The composition of the diatom fluxes was similar for every year sampled at BR-G while it varied between years at BR-1 and BR-3. Although diatom community composition usually remained similar throughout the bloom at BR-G and BR-3, unidentified pennate diatoms and the centric diatom *Chaetoceros* spp. first dominated diatom fluxes at the beginning of July at BR-1, followed by a predominance of the centric diatom *Thalassiosira* spp. and of the pennate diatom *Licmophora* spp. during late summer in 2013. In 2017, a majority of *Chaetoceros* spp. recorded in diatom fluxes at the end of June was followed by a majority of the centric diatom *Skeletonema* spp. in summer August 2017 (Fig. 7).

When present, maximum fluxes of the sea ice-obligated algae *Nitzschia frigida* ranged from ~500 cells m⁻² d⁻¹ at BR-3 in June 2017 to ~1.8 million cells m⁻² d⁻¹ at BR-G in early May 2015 (Fig. 8). *N. frigida* was absent at BR-1 in 2013 and at BR-3 in 2014, while empty cells only were collected at BR-G in 2017. Maximum *N. frigida* fluxes were observed nearly simultaneously at the two southernmost locations, with the earliest maximums observed in late April 2016 and the latest maximums observed in late June 2013. At BR-3, maximums in *N. frigida* fluxes were recorded in June 2016 and 2017, ten and four weeks later than at the southernmost sites (Fig. 8). The freshwater-associated pennate diatom group *Asterionella/Diatoma* spp. was present only at BR-1, with fluxes recorded in July and August 2015 and 2017 and in October 2016 (Fig. 8).

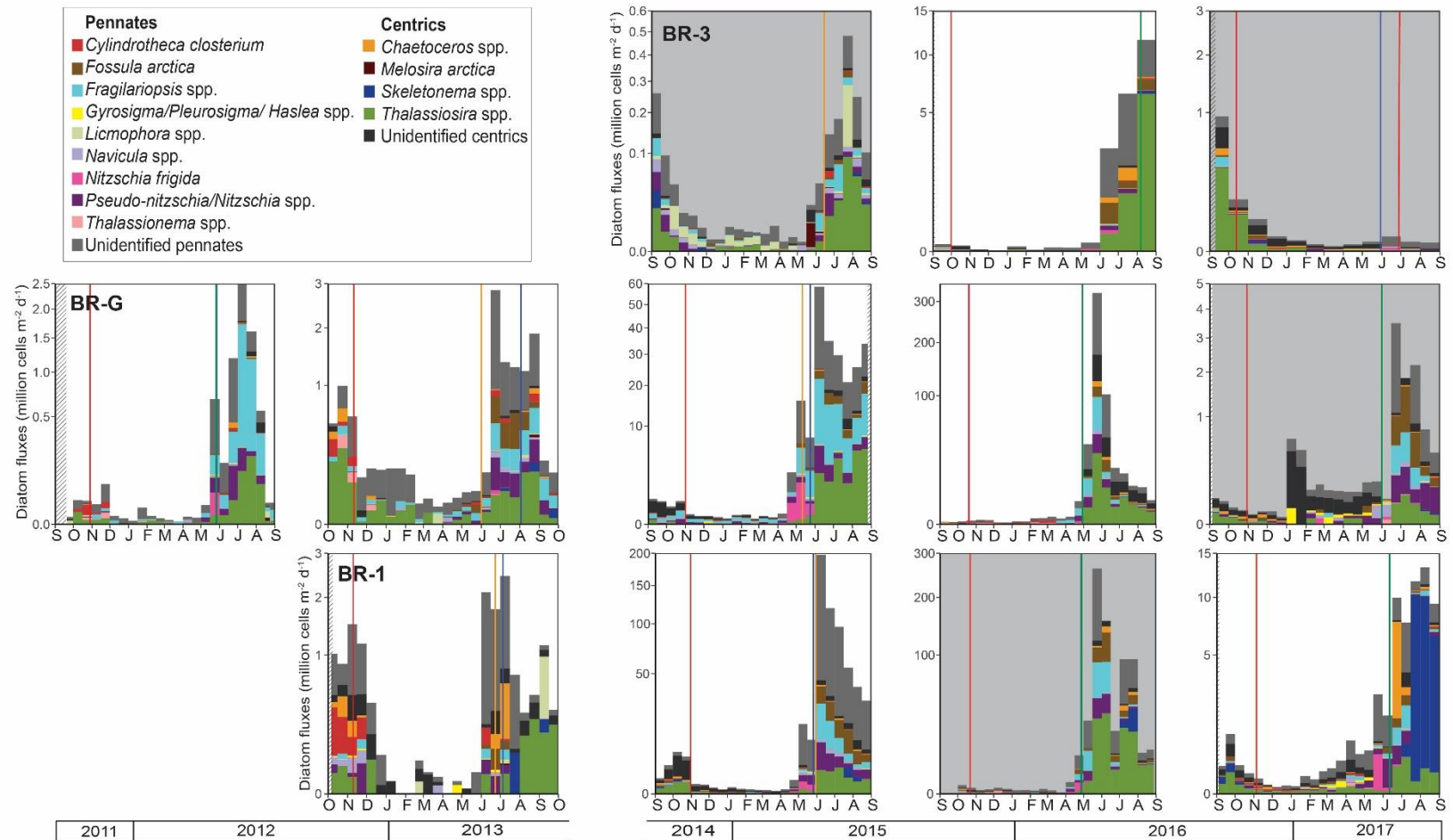


Figure 7: Fluxes of the 15 most abundant diatom groups at the three mooring sites. Panels with grey backgrounds show deployment under 300 m. Note the different scales.

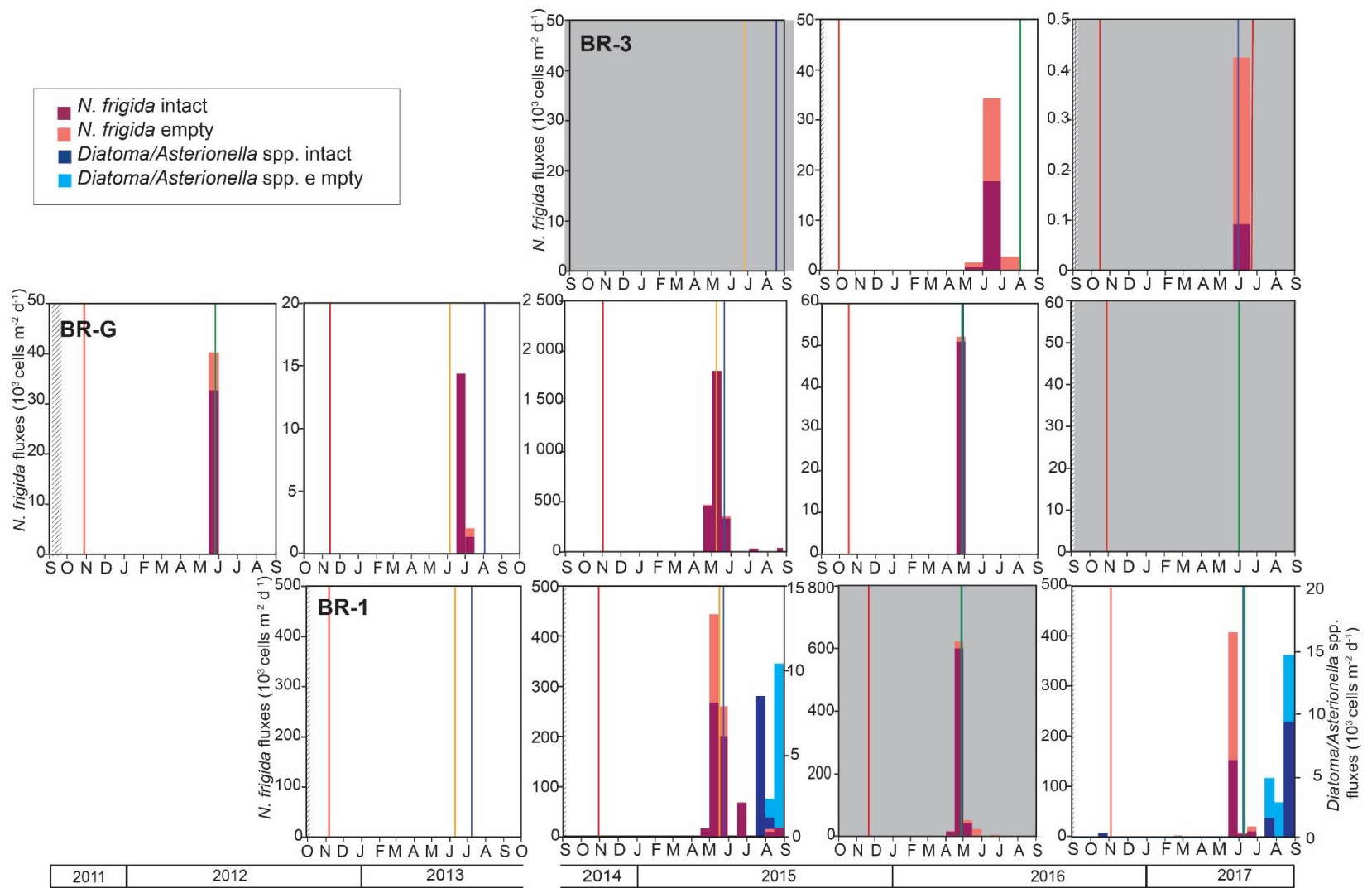


Figure 8: Fluxes of the ice-obligated diatom *Nitzschia frigida* and the freshwater diatom group *Diatoma/Asterionella* spp. at the three mooring sites. Panels with grey backgrounds show deployments under 300 m.

4.4 Seasonal and annual diatom and MC fluxes

Spring-summer diatom fluxes ranged from ~0.1 million cells m⁻² at BR-3 in 2017 to ~12500 million cells m⁻² at BR-1 in 2016, while autumn fluxes ranged from ~0.25 million cells m⁻² at BR-3 in 2015 to ~200 million cells m⁻² at BR-1 in 2014 (Fig. 9a). Unidentified pennate diatoms often dominated diatom fluxes, especially during spring-summer (Fig. 9a and b). Centric diatoms *Chaetoceros* spp. and *Thalassiosira* spp. and the cold-water associated pennate diatom *Fragilariopsis* spp. were among the most abundant groups for all seasons and sites (Fig. 6a and b). At the two southernmost sites, *Cylindrotheca closterium* was generally abundant during autumn while the cold-water associated *Fossula arctica* was abundant during spring-summer. A large proportion of the autumn fluxes was often dominated by unidentified centric diatoms (Fig. 9a and b). While rarely present at BR-3 and BR-G, *Skeletonema* spp. was recorded at BR-1 and dominated spring-summer fluxes in 2017. At BR-3, *Licmophora* spp. was particularly abundant during autumn 2014 and 2015 and during spring-summer 2015 (Fig. 9a and b).

Spring-summer MC fluxes ranged from ~0.05 mg C m⁻² at BR-3 in 2017 to ~500 mg C m⁻² at BR-1 in 2016, while autumn fluxes ranged from ~0.05 mg C m⁻² at BR-3 in 2015 to ~1.4 mg C m⁻² at BR-1 in 2014 (Fig. 9c). Due to their large volumes, *Thalassiosira* spp. and *Licmophora* spp. contributed to most of the MC fluxes at the two southernmost sites and at BR-3, respectively (Fig. 9c and d). Annual MC fluxes ranged from 1 mg C m⁻² yr⁻¹ for the 2016-2017 cycle at BR-3 to 520 mg C m⁻² yr⁻¹ for the 2015-2016 cycle at BR-1 (Table 2). The highest proportion of MC to the annual POC flux was recorded for the 2015-2016 cycle at all sites (Table 2).

Table 2. Annual microalgal carbon (MC) and contributions of MC to the POC fluxes (in parentheses, in %) at the three sites. Grey cells show deployment under 300 m.

	Annual MC flux (mg C m ⁻² yr ⁻¹)				
	2011-2012	2012-2013	2014-2015	2015-2016	2016-2017
BR-3			2 (0.7)	13 (1.8)	1 (0.2)
BR-G	4(0.2)	4 (0.2)	103 (3.1)	410 (9.1)	5 (0.1)
BR-1		14 (0.2)	204 (3.3)	520 (10.8)	14 (0.3)

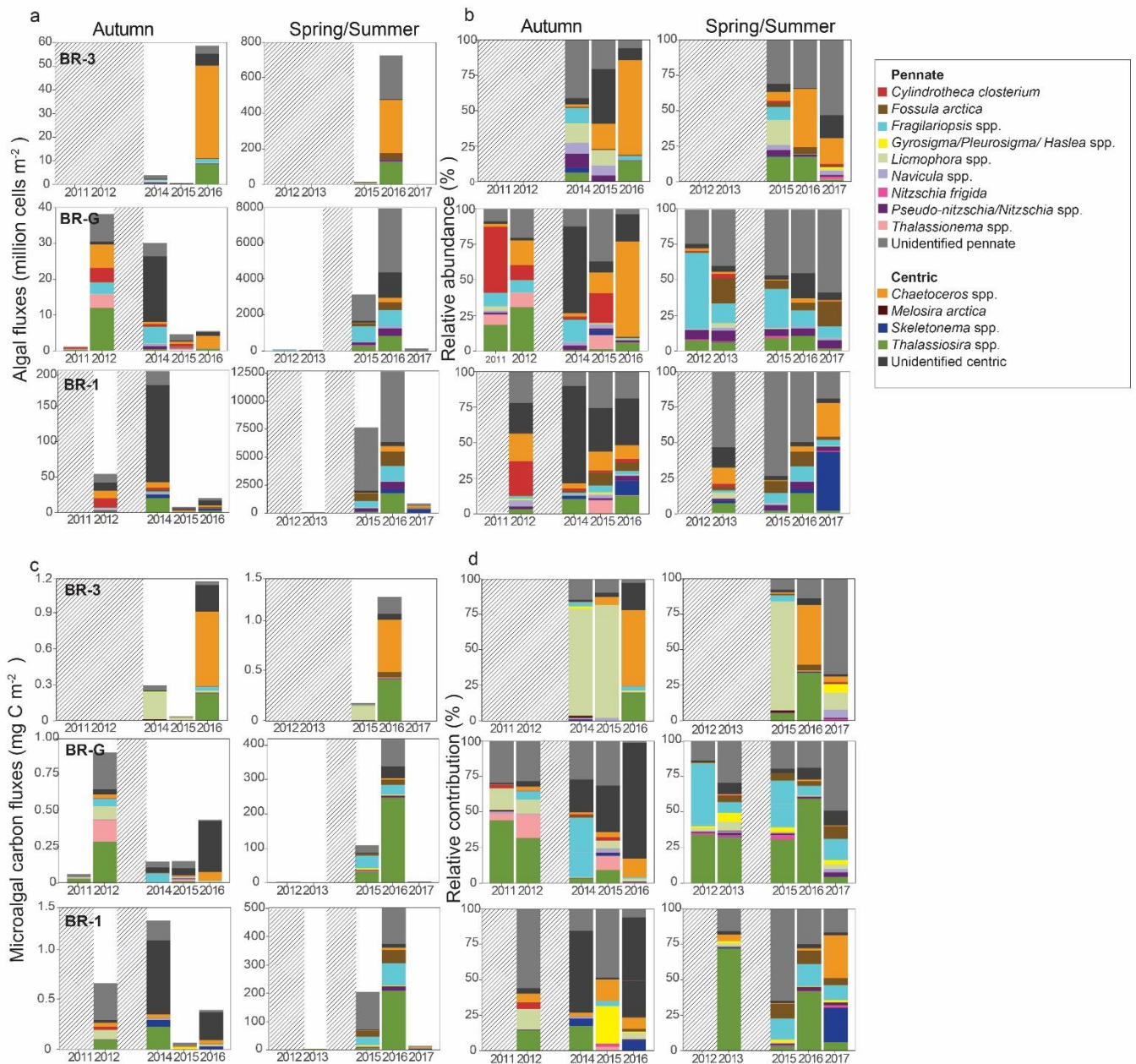


Figure 9: Absolute (a) and relative (b) microalgal fluxes and absolute (c) and relative (d) microalgal carbon fluxes for autumn (September to November) and spring/summer (April to August) for the 15 most abundant diatoms groups collected at the three mooring sites.

5. Discussion

Diatom cells (intact, empty and spores) contributed to >75% of the annual microalgal fluxes in the Beaufort Sea. Small-size microalgal groups such as silicoflagellates, coccolithophores and flagellates contributed to <25% of the annual microalgal fluxes and represented a significant proportion of the microalgal flux only during periods of low fluxes. Diatoms dominate microalgal abundance, biomass, and diversity during spring in the Arctic Ocean (Booth and Horner, 1997; Gosselin et al., 1997; Von Quillfeldt, 2000; Werner et al., 2007; Degerlund and Eilertsen, 2010; Poulin et al., 2011), while flagellates usually dominate microalgal abundance during autumn (Juul-Pedersen et al., 2010; Ardyna et al., 2011; Blais et al., 2017). The prymnesiophyte *Phaeocystis pouchetii* also occasionally dominates microalgal abundance, mostly in the Atlantic-influenced waters of the Arctic Ocean (Reigstad and Wassmann, 2007; Degerlund and Eilertsen, 2010; Assmy et al., 2017; Wollenburg et al., 2018). Due to their heavy silicate frustules, diatoms sink faster than small-sized microalgal groups, with sinking rates ranging from 100 to 150 m d⁻¹ (Turner, 2002). In contrast, distinct physical processes are typically required for the export of small cells at depth, as suggested by observations in Fram Strait and the Eurasian Arctic Ocean (Lalonde et al., 2011; Lalonde et al., 2019). Therefore, while microalgal fluxes obtained at depths ranging between ~125 and ~300 m in the Beaufort Sea only partly reflected the overlying microalgal community, diatom fluxes reflected the magnitude, timing and composition of the diatom blooms.

5.1. Impact of early snowmelt and sea ice break-up

Over the Mackenzie shelf break (BR-G and BR-1), snowmelt and sea ice break-up occurred at least one month earlier in 2016 than during other years sampled, leading to earlier sea ice algae release, earlier peak in diatom fluxes, highest spring-summer diatom fluxes, and the largest contribution of MC to the POC fluxes at both sites. Sea ice and snow conditions further north off Banks Island (BR-3) were heavier than those at the Mackenzie shelf break, with the recurrence of pluriannual ice over the mooring site (Fig. 4). Using the 50% sea ice concentration threshold, sea ice break-up occurred earlier in 2017 than in 2016 over the

Banks shelf. However, 2016 was the only year with prolonged ice-free conditions, reflecting the regional decline in sea ice cover in Beaufort Sea. This sustained open water period also led to earlier sea ice algae release, earlier peak in diatom fluxes, highest spring-summer diatom fluxes, and the largest contribution of MC to the POC fluxes over Banks shelf, similar to observations over the Mackenzie shelf.

The early onset of snowmelt in late April 2016 over the Mackenzie shelf and the prolonged ice-free conditions over the Banks shelf led to an early release of ice algae, reflected by the collection of *N. frigida* in the sediment traps. The ice-obligated chain-forming pennate diatom *N. frigida* is widely distributed in the Arctic Ocean (Poulin et al., 2011; Szymanski and Gradinger, 2016) and its net-like structure is well-suited for aggregation and rapid sedimentation (Michel et al., 1993). The onset of snowmelt has been reported to trigger the release of sea ice algae in the Arctic Ocean (Welch and Bergmann, 1989; Cota and Smith, 1991; Fortier et al., 2002). Accordingly, *N. frigida* was consistently among the first diatom species exported, similar to previous diatom flux measurements in the Beaufort Sea and in the Eurasian Arctic Ocean (Dezutter et al., 2019; Lalande et al., 2019). The early snowmelt and sea ice algae release observed in 2016 likely affected the sympagic and benthic communities through an earlier availability of food after winter depletion.

The early onset of snowmelt and sea ice break-up over the Mackenzie shelf and the prolonged ice-free conditions over the Banks shelf in 2016 led to an earlier peak in diatom fluxes in the Beaufort Sea. Diatom fluxes first increased under-ice during snowmelt and reached their maximum values shortly after sea ice break-up, showing a clear correlation between the timing of the peak in diatom flux and the dates of snowmelt and sea ice break-up (Fig. 10a and b). In the Arctic Ocean, phytoplankton blooms are triggered by increased irradiance and stratification resulting from sea ice melt (Hsiao, 1992; Fortier et al., 2002). Hence, early snowmelt and sea ice break-up over the Mackenzie shelf and the reduced ice conditions over the Banks shelf in 2016 led to earlier light availability and stratification in the upper water column, allowing an earlier pelagic microalgal bloom reflected by peaks in diatom fluxes one month earlier than for other years sampled. These early peaks in diatom fluxes likely affected the seasonal development of the herbivorous zooplankton community by providing

an earlier food supply or on the other hand, depriving them of the resource needed migrating upward, out of their winter dormancy.

The early onset of snowmelt over the Mackenzie shelf and the prolonged ice-free conditions over the Banks shelf in 2016 also led to the highest spring-summer diatom and MC fluxes, at least two times higher than for other years sampled at any site in the Beaufort Sea (Fig. 9). While remote sensing observations attributed an increase in primary production to a reduced sea ice extent in early summer (Kahru et al., 2011), diatom fluxes indicated that early snowmelt also played a determining role to enhance microalgal fluxes, as reflected by the correlations between spring-summer diatom and MC fluxes with the timing of snowmelt and sea ice break-up (Fig. 11). Remote sensing-derived observations also suggested that the enhanced primary production observed in several regions of the Arctic Ocean was the result of a longer open water period (Arrigo and van Dijken, 2015). However, the highest spring-summer diatom and MC fluxes in 2016 were not the result of a longer productive period, with diatom fluxes >10 million cells $\text{m}^{-2} \text{d}^{-1}$ recorded over a period of ~ 10 weeks compared to a sustained productive period of ~ 14 weeks over the Mackenzie shelf in 2015 (Fig. 6).

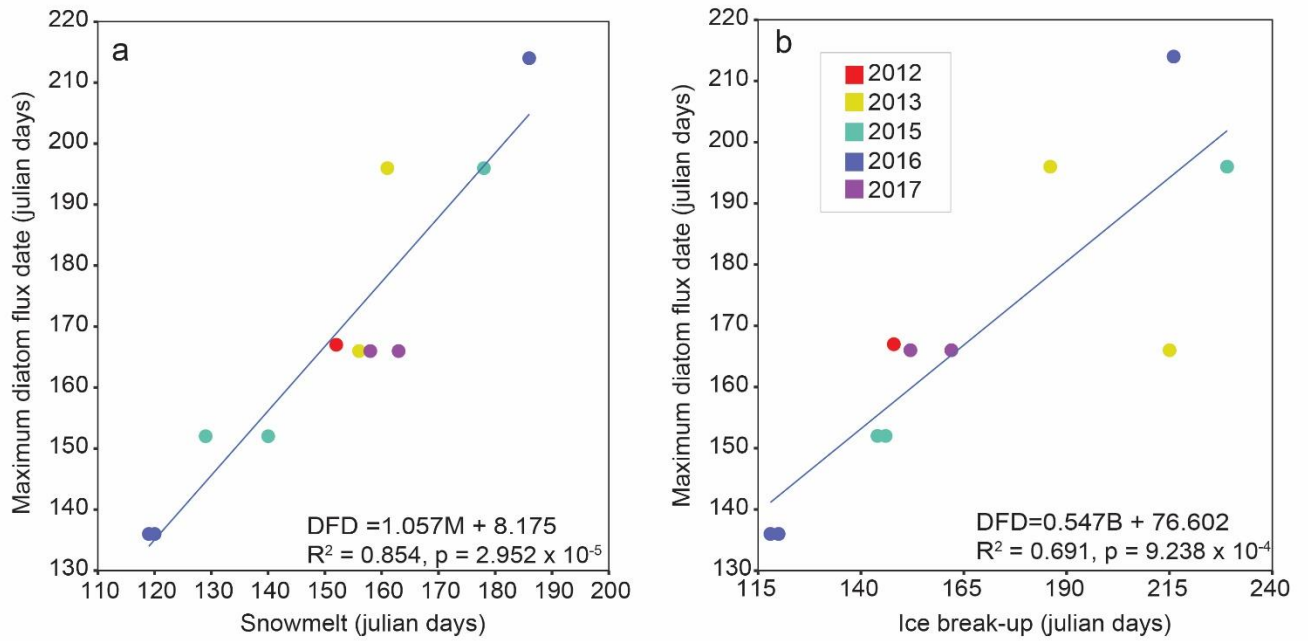


Figure 10: Correlation between (a) the onset of snowmelt (M) and the dates of maximum diatom flux (DFD) using the first day of collection period, and (b) the date of sea ice break-up (B) and the dates of maximum diatom flux using the first day of collection period.

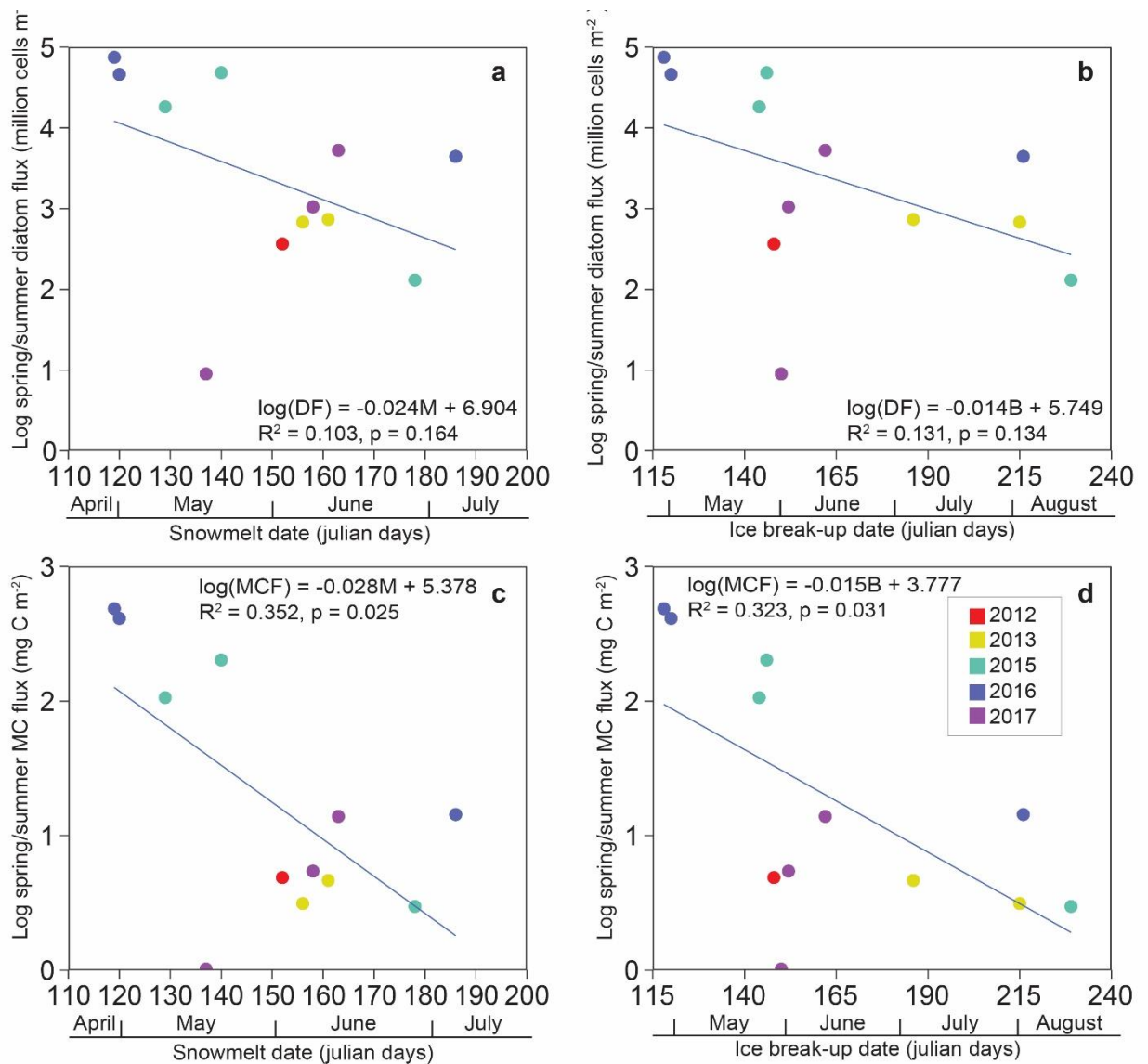


Figure 11: Correlation between (a) the onset of snowmelt (M) and the spring/summer diatom fluxes (DF), (b) the date of sea ice break-up (B) and the spring/summer diatom fluxes, (c) the onset of snowmelt and the spring/summer MC fluxes (MCF), and (d) the date of sea ice break-up and the spring/summer MC fluxes. Regression equations are given with the p value of the slope and marginal r^2 .

The highest diatom and MC fluxes recorded in 2016 may have reflected enhanced algal growth in surface waters and/or reduced zooplankton grazing at the onset of the bloom in late April. Females of the key Arctic grazer *Calanus glacialis* utilize the ice algae bloom to fuel early maturation and reproduction, whereas their nauplii feed on the phytoplankton bloom (Søreide et al., 2010; Leu et al., 2011). In the Amundsen Gulf, the large herbivorous copepod *Calanus hyperboreus* usually overwinter in the relatively warm ($\sim 0^{\circ}\text{C}$) Atlantic layer below 200 m and migrate upward the following spring to feed on the ice algae bloom (Darnis and Fortier, 2014). The temporal lag between the microalgal bloom and the migration and development of the *Calanus* community reduces grazing efficiency, as demonstrated by model results showing that an early diatom bloom in March, before the upward migration of copepods, led to a 57% increase in primary production in Western Greenland (Hansen et al., 2003). A delayed upward migration of *C. glacialis* after the ice algae bloom may lead to a lower reproductive success and therefore to a lower grazing pressure of *C. glacialis* nauplii on the phytoplankton bloom. The highest diatom fluxes observed following an early sea ice break-up are likely the result of a mismatch between the microalgal blooms and grazing by herbivorous copepods.

The largest contribution of MC to the POC fluxes in the Beaufort Sea in 2016 support the export of a larger proportion of diatoms before strong grazing pressure by herbivorous copepods, thus decreasing the retention of carbon at the surface and favoring pelagic-benthic coupling (Table 2). Although the contribution of MC to POC fluxes were the highest recorded in 2016, MC fluxes contributed to a maximum of 11 % of the annual POC fluxes at 306 m, indicating that intact ungrazed diatom cells are not the main contributors to carbon export in the Beaufort Sea, even during the case of an early bloom, as showed by field measurement and inverse modeling analyses in the Amundsen Gulf (Forest et al., 2011). Similarly, short-term sediment traps deployed over the Mackenzie Shelf during early spring reported that 38% of the POC sinking flux at 25 m was due to algal cells (Juul-Pedersen et al., 2008), while moored sediment traps deployed in the Eurasian Arctic Ocean reported that 0.7 to 14.5% of the annual POC sinking flux at ~ 200 m was due to algal cells (Lalande et al., 2019).

5.2. Impact of late snowmelt and sea ice break-up

The record sea ice minimum extent of September 2012 was followed by a nearly 50 % increase in Arctic sea ice extent in September 2013 due to a variety of factors including ice dynamics, wind, oceanic and heat transport, solar insolation anomalies, and below-average winter Arctic cloud cover (Liu and Key, 2014; Serreze and Stroeve, 2015). Most of the 2013 rebound in sea ice cover occurred in the Beaufort Sea (Liu and Key, 2014), leading to late snowmelt and sea ice break-up above both mooring sites sampled that year over the Mackenzie shelf. Snowmelt occurred more than two weeks later while sea ice break-up occurred at least one month later than during other years sampled. This late snowmelt and sea ice break-up led to a late sea ice algae release and to the lowest spring-summer diatom and MC fluxes over the Mackenzie shelf. Similar trends of late sea ice algae release, low diatom fluxes, and MC fluxes were observed off Banks Island, where heavy ice conditions often led to late snowmelt and sea ice break-up several weeks later than the Mackenzie shelf sites.

The delayed snowmelt led to a one-month delay in the release of ice algae at BR-G, as reflected by *N. frigida* fluxes. Although *N. frigida* cells were not observed in the sediment trap at BR-1, sea ice algae release in the region likely occurred at the onset of snowmelt at the end of June. In contrast, a peak in diatom fluxes was observed in mid-June at BR-G, before the late sea ice break-up observed in August, reflecting an under-ice pelagic bloom following snowmelt and a limited influence of the delayed sea ice break-up on diatom export. A similar trend of under-ice enhanced diatom export was observed at BR-1, although a peak in diatom export was observed shortly after sea ice break-up. The occurrence of under-ice pelagic blooms was reflected by the export of the centric diatom *Chaetoceros* spp., a genus that often dominates pelagic blooms in the Beaufort Sea and on Arctic continental shelves (Gran, 1900; Von Quillfeldt, 2000; Degerlund and Eilertsen, 2010; Juul-Pedersen et al., 2010). The delayed snowmelt led to the simultaneous release of ice algae and peak in diatom fluxes instead of the release of ice algae usually observed one to two months before the peak in diatom fluxes. The delayed snowmelt of 2013 led to a mismatch between the upward migration of *C. glacialis* females and sea ice algae release and to a negative impact on their reproduction and recruitment, as indicated by the fewer *C. glacialis* nauplii collected in

the sediment trap at BR-G in June and July 2013 than during five other years sampled at the same site (Dezutter et al., 2019). As *C. glacialis* nauplii constitute an important food source for polar cod larvae (Michaud et al., 1996; Benoit et al., 2010), a lower abundance of *Calanus* nauplii in 2013 had the potential to reduce populations of copepods, polar cod larvae and polar cod adults in the Beaufort Sea. Indeed, lower epipelagic polar cod larvae and mesozooplankton biomass derived from a Simrad echosounder mounted on the CCGS *Amundsen* were measured in 2013 than during five other years sampled in the Beaufort Sea (LeBlanc et al., 2019).

The late snowmelt and sea ice break-up in 2013 also led to the lowest spring-summer diatom and MC fluxes recorded over the Mackenzie shelf. Reduced light availability likely led to the lower fluxes observed in 2013, as sea ice cover restrain light transmittance (Nicolaus et al., 2012). Similar to results obtained in 2013 over the Mackenzie shelf, diatom and MC fluxes recorded off Banks Island were relatively low due to the delayed snowmelt and sea ice break-up. The higher proportion of diatom resting spores collected in microalgal fluxes off Banks Island also suggest that the area is nutrient-limited, as resting spores are usually formed in the last phase of diatom blooms and regarded as means of protection against unfavorable conditions (Hegseth and Sundfjord, 2008).

5.3. Impact of a late sea ice freeze-up

Late sea ice freeze-ups were observed in mid-November 2012 and 2014 over the Mackenzie shelf, two weeks later than for the other years sampled, leading to autumn diatom fluxes of similar range than low spring/summer fluxes. However, no correlation was observed between the date of sea ice freeze-up and the magnitude of the autumn fluxes ($r^2 = 0.24$, $n = 10$, data not shown). A late sea ice freeze-up and a longer exposition of surface waters to wind stress have been reported to increase the frequency of satellite-derived autumn blooms from 11% (1998–2001) to 15% (2007–2012) in the Beaufort Sea due to the replenishment of nutrients following water column mixing (Ardyna et al., 2014). *In situ* measurements also showed enhanced microalgal production associated with upwelling-favorable winds during October 2007 in the coastal Beaufort Sea (Tremblay et al., 2011). The same process likely explained the higher diatom fluxes observed during autumn in 2012 and 2014. Although autumn blooms in the Beaufort

Sea are generally dominated by a flagellate-based community (Juul-Pedersen et al., 2010; Ardyna et al., 2011), an increase in the contribution of diatoms to the autumn microalgal community was reported recently for the region (Blais et al., 2017). Although autumn diatom fluxes were two orders of magnitude lower than the highest spring-summer fluxes recorded in 2016, these enhanced diatom fluxes contributed to a higher POC export to the seafloor and have the potential to increase sequestration of algal carbon in the Arctic Ocean.

The species dominating the composition of the spring/summer diatom fluxes in 2013 and 2016 were similar than for other years sampled, despite the late and early snowmelt and sea ice break-up. Similarly, the composition of the autumn diatom fluxes was similar for all years sampled. In contrast, the species composing the autumn diatom fluxes were different than during spring-summer over the Mackenzie shelf. While *Fossula arctica* was prevalent during spring-summer, the pennate diatom *Cylindrotheca closterium* was prevalent during autumn (Fig. 9).

5.4. Influence of the Mackenzie River

The Mackenzie River has the fourth largest runoff in the Arctic Ocean, with the maximum discharge observed in June (Carmack and Macdonald, 2002). In the absence of strong winds, the Mackenzie plume will flow along the Tuktoyaktuk Peninsula toward Amundsen Gulf due to the Coriolis effect. Winds from the east may push the Mackenzie plume northward on the Mackenzie shelf, occasionally reaching the BR-1 site (Forest et al., 2007). Fluxes of the freshwater diatom group *Diatoma/Asterionella* spp. reflected the expansion of the Mackenzie River plume over the BR-1 site during summer in 2015 and 2017. The absence of *Diatoma/Asterionella* spp. in 2013 and 2016 suggest that a restricted expansion of the plume compared to the other years sampled.

6. Conclusion

The nearly continuous record of microalgal fluxes obtained in the Beaufort Sea from 2011 to 2017 reflected a change in the timing and magnitude of diatom fluxes in relation to snow and sea ice cover. As global climate warms, increasingly earlier snowmelt and sea ice break-up are expected, potentially leading to earlier ice algae release and earlier and higher microalgal spring/summer fluxes, as suggested from diatom fluxes recorded in 2016. As the enhanced diatom fluxes observed following the early sea ice break-up likely resulted

from a mismatch between phytoplankton bloom and zooplankton grazing pressure, increasingly earlier snow and sea ice melt are likely to increase carbon export from ungrazed diatom cell to the seafloor and its potential sequestration. In addition, increasingly late sea ice freeze-up may lead to recurring autumn blooms and enhanced diatom fluxes. On the other hand, rebounds in sea ice cover following a year of low sea ice extent, as observed in 2013, may lead to lower diatom fluxes as well as reduced pelagic-benthic coupling and carbon sequestration. Both these scenarios highlight the strong dependence of microalgal growth and export to the timing of snowmelt, sea ice break-up and sea ice freeze-up and their subjectivity to change in a context of climate change. Overall, these results also highlight the importance of long-term observations to accurately monitor the impact of the changing snow and sea ice cover on the Arctic marine ecosystems.

7. Acknowledgments

We thank the officers and crew of the CCGS *Amundsen* and CCGS *Sir Wilfrid Laurier* and all mooring technicians involved in the deployment and recovery of moorings. We also thank Thibaud Dezutter for ice and snow cover data, and Marie Parenteau and Eva-Maria Nöthig for taxonomic analyses and advices.

8. Funding

This work was supported by the Long-Term Oceanic Observatories (LTOO) project funded by the Network of Centres of Excellence of Canada ArcticNet. Logistical support was provided by the Amundsen Science program funded through the Canada Foundation for Innovation. G.N. was supported by a Natural Sciences and Engineering Research Council of Canada Alexander Graham Bell Canada Graduate Scholarship and by the Fonds de recherche Nature et Technologies du Québec.

Conclusion générale

L'Océan Arctique subit présentement d'importants changements dans son régime de glace et de neige en raison du réchauffement climatique. Ces changements affectent l'ensemble de l'écosystème, en particulier les microalgues, organismes à la base du réseau trophique. Il est donc impératif d'observer de façon continue et à long terme cet environnement unique afin de comprendre comment l'écosystème marin réagit face à ces changements.

Dans cette étude, des pièges à particules déployés de 2011 à 2017 ont servi à observer les changements dans le timing, l'abondance et la composition de l'export des microalgues dans la mer de Beaufort en réponse aux changements dans le régime de neige et de glace. L'utilisation de pièges à particules, combinée à l'utilisation de données de concentration de glace et d'épaisseur du couvert de neige obtenues à partir d'images satellites, nous a permis d'obtenir des séries temporelles uniques pour des variables physiques et biologiques qui n'auraient pu être décrites avec des méthodes d'échantillonnage conventionnelles.

Puisque les diatomées dominent les floraisons printanières dans l'océan Arctique et qu'elles coulent plus rapidement que les groupes de microalgues de petite taille en raison de leurs frustules de silice, les cellules microalgales récoltées dans les pièges reflètent indirectement la dynamique de la production primaire en surface. Les pièges à particules ont permis de documenter les cycles annuels d'export des microalgues et particulièrement d'observer l'export printanier débutant sous la glace, puis atteignant son maximum peu après la débâcle. De plus, il a été possible de comprendre la relation étroite entre le relâchement des algues de glace et la fonte du couvert de neige sur la banquise, reflétée par l'export de *N. frigida*, une pennée exclusivement associée à la glace. L'influence du panache de la rivière Mackenzie à BR-1 a aussi pu être observée, reflétée par l'export des diatomées d'eau douce *Diatoma/Asterionella* spp. Les floraisons pélagiques ont été reflétées par l'export de la centrique *Chaetoceros* spp.

En 2016, la fonte du couvert de neige et la débâcle des glaces de mer ont eu lieu au moins un mois avant les autres années échantillonnées. La fonte hâtive du couvert de neige et de glace de mer a entraîné la libération des algues de glace et le maximum d'export de diatomées plus tôt, des flux de diatomées printemps-été plus élevés et une plus grande proportion de MC dans le flux de POC aux 3 sites échantillonnés. Cette augmentation drastique de l'export saisonnier de microalgues peut être due à l'augmentation de la période de croissance engendrée par la fonte hâtive du couvert de glace et de neige et à l'export vertical des cellules échappant au broutage par le zooplancton. Dans une étude ultérieure, il serait intéressant de mesurer les flux de pelotes fécales afin de confirmer cette dernière hypothèse. L'obtention de données de nutriments permettrait de confirmer la disponibilité et l'utilisation des nutriments par les microalgues lorsque la floraison survient plus tôt. La réponse de l'export de microalgues en réponse à une fonte du couvert de neige et de glace de mer hâtive peut nous servir d'exemples concrets de ce à quoi pourrait ressembler la dynamique de l'écosystème dans un avenir rapproché si la tendance dans la réduction du couvert de glace arctique se maintient.

En 2013, des conditions de glace anormales ont entraîné une fonte du couvert de neige et de glace tardive dans la mer de Beaufort. Cette fonte tardive a entraîné un relâchement tardif des algues de glace dans la colonne d'eau et des flux printemps-été de diatomées et de MC plus petits. Cette diminution peut avoir des conséquences négatives sur le transfert d'énergie dans la chaîne trophique.

La formation tardive du couvert de glace à la mi-novembre 2012 et 2014 à BR-G et à BR-1, contrairement à la fin octobre, a entraîné un export substantiel de diatomées en automne, juste avant la formation du couvert de glace. Ces résultats confirment les observations d'Ardyna et al. (2014) sur l'apparition de plus en plus fréquente des floraisons automnales en Arctique. Cette prolongation de la production primaire représente un apport de carbone supplémentaire pour le réseau trophique.

Ces séries temporelles continues sont l'une des rares mesures de la communauté de microalgues qui incluent le début de la période productive. Ces résultats permettent de mieux comprendre la dynamique des microalgues dans la mer de Beaufort et les tendances prévisibles dans des conditions plus chaudes dans l'océan Arctique. Des mesures à long terme sont essentielles pour surveiller l'impact de la réduction du couvert de glace de mer sur l'écosystème. En dépit des contraintes, il est primordial de poursuivre le déploiement de mouillages et de pièges à particules comme outils d'échantillonnage à long terme, car ils permettent d'obtenir des banques de données essentielles pour l'étude de plusieurs variables de l'écosystème et c'est avec des initiatives comme le projet LTOO qu'il sera réellement possible de mesurer les impacts à long terme des changements climatiques sur l'océan Arctique.

Bibliographie

- ACIA. 2004. Impacts of a Warming Arctic-Arctic Climate Impact Assessment. Impacts of a Warming Arctic-Arctic Climate Impact Assessment, by Arctic Climate Impact Assessment, pp. 144. ISBN 0521617782. Cambridge, UK: Cambridge University Press, December 2004.:144.
- Ardyna, M., M. Babin, M. Gosselin, E. Devred, L. Rainville, and J. É. Tremblay. 2014. Recent Arctic Ocean sea ice loss triggers novel fall phytoplankton blooms. *Geophysical Research Letters* **41**:6207-6212.
- Ardyna, M., M. Gosselin, C. Michel, M. Poulin, and J.-É. Tremblay. 2011. Environmental forcing of phytoplankton community structure and function in the Canadian High Arctic: contrasting oligotrophic and eutrophic regions. *Marine Ecology Progress Series* **442**:37-57.
- Arrigo, K. R., D. K. Perovich, R. S. Pickart, Z. W. Brown, G. L. Van Dijken, K. E. Lowry, M. M. Mills, M. A. Palmer, W. M. Balch, and F. Bahr. 2012. Massive phytoplankton blooms under Arctic sea ice. *Science* **336**:1408-1408.
- Arrigo, K. R., G. van Dijken, and S. Pabi. 2008. Impact of a shrinking Arctic ice cover on marine primary production. *Geophysical Research Letters* **35**.
- Arrigo, K. R., and G. L. van Dijken. 2015. Continued increases in Arctic Ocean primary production. *Progress in Oceanography* **136**:60-70.
- Assmy, P., M. Fernández-Méndez, P. Duarte, A. Meyer, A. Randelhoff, C. J. Mundy, L. M. Olsen, H. M. Kauko, A. Bailey, and M. Chierici. 2017. Leads in Arctic pack ice enable early phytoplankton blooms below snow-covered sea ice. *Scientific reports* **7**:40850.
- Babb, D., R. Galley, D. Barber, and S. Rysgaard. 2016. Physical processes contributing to an ice free Beaufort Sea during September 2012. *Journal of Geophysical Research: Oceans* **121**:267-283.
- Benoit, D., Y. Simard, J. Gagné, M. Geoffroy, and L. Fortier. 2010. From polar night to midnight sun: photoperiod, seal predation, and the diel vertical migrations of polar cod (*Boreogadus saida*) under landfast ice in the Arctic Ocean. *Polar Biology* **33**:1505-1520.
- Blais, M., M. Ardyna, M. Gosselin, D. Dumont, S. Bélanger, J. É. Tremblay, Y. Gratton, C. Marchese, and M. Poulin. 2017. Contrasting interannual changes in phytoplankton productivity and community structure in the coastal Canadian Arctic Ocean. *Limnology and Oceanography* **62**:2480-2497.
- Boetius, A., S. Albrecht, K. Bakker, C. Bienhold, J. Felden, M. Fernández-Méndez, S. Hendricks, C. Katlein, C. Lalande, and T. Krumpfen. 2013. Export of algal biomass from the melting Arctic sea ice. *Science* **339**:1430-1432.
- Booth, B. C., and R. A. Horner. 1997. Microalgae on the Arctic Ocean Section, 1994: species abundance and biomass. *Deep Sea Research Part II: Topical Studies in Oceanography* **44**:1607-1622.
- Budge, S., M. Wooller, A. Springer, S. J. Iverson, C. McRoy, and G. Divoky. 2008. Tracing carbon flow in an arctic marine food web using fatty acid-stable isotope analysis. *Oecologia* **157**:117-129.
- Campbell, K., C. Mundy, D. Barber, and M. Gosselin. 2015. Characterizing the sea ice algae chlorophyll a–snow depth relationship over Arctic spring melt using transmitted irradiance. *Journal of Marine Systems* **147**:76-84.
- Carmack, E., and D. C. Chapman. 2003. Wind-driven shelf/basin exchange on an Arctic shelf: The joint roles of ice cover extent and shelf-break bathymetry. *Geophysical Research Letters* **30**.
- Carmack, E. C., and R. W. Macdonald. 2002. Oceanography of the Canadian Shelf of the Beaufort Sea: A Setting for Marine Life. *Arctic* **55**:29-45.

- Carmack, E. C., R. W. Macdonald, and J. E. Papadakis. 1989. Water mass structure and boundaries in the Mackenzie shelf estuary. *Journal of Geophysical Research: Oceans* **94**:18043-18055.
- Christensen, J. H., and O. B. Christensen. 2003. Climate modelling: severe summertime flooding in Europe. *Nature* **421**:805-806.
- Cota, G. F., and R. E. Smith. 1991. Ecology of bottom ice algae: III. Comparative physiology. *Journal of Marine Systems* **2**:297-315.
- Darnis, G., and L. Fortier. 2014. Temperature, food and the seasonal vertical migration of key arctic copepods in the thermally stratified Amundsen Gulf (Beaufort Sea, Arctic Ocean). *Journal of Plankton Research* **36**:1092-1108.
- Darnis, G., D. Robert, C. Pomerleau, H. Link, P. Archambault, R. J. Nelson, M. Geoffroy, J.-É. Tremblay, C. Lovejoy, S. H. Ferguson, B. P. V. Hunt, and L. Fortier. 2012. Current state and trends in Canadian Arctic marine ecosystems: II. Heterotrophic food web, pelagic-benthic coupling, and biodiversity. *Climatic Change* **115**:179-205.
- Degerlund, M., and H. C. Eilertsen. 2010. Main species characteristics of phytoplankton spring blooms in NE Atlantic and Arctic waters (68–80 N). *Estuaries and Coasts* **33**:242-269.
- Dezutter, T., C. Lalande, C. Dufresne, G. Darnis, and L. Fortier. 2019. Mismatch between microalgae and herbivorous copepods due to the record sea ice minimum extent of 2012 and the late sea ice break-up of 2013 in the Beaufort Sea. *Progress in Oceanography* **173**:66-77.
- Edler, L. 1979. Recommendations on methods for Marine Biological Studies in the Baltic Sea. Phytoplankton and Chlorophyll. . Baltic Marine Biologists Publication No. 5:38.
- Forest, A., M. Sampei, H. Hattori, R. Makabe, H. Sasaki, M. Fukuchi, P. Wassmann, and L. Fortier. 2007. Particulate organic carbon fluxes on the slope of the Mackenzie Shelf (Beaufort Sea): Physical and biological forcing of shelf-basin exchanges. *Journal of Marine Systems* **68**:39-54.
- Forest, A., J.-É. Tremblay, Y. Gratton, J. Martin, J. Gagnon, G. Darnis, M. Sampei, L. Fortier, M. Ardyna, and M. Gosselin. 2011. Biogenic carbon flows through the planktonic food web of the Amundsen Gulf (Arctic Ocean): A synthesis of field measurements and inverse modeling analyses. *Progress in Oceanography* **91**:410-436.
- Fortier, M., L. Fortier, C. Michel, and L. Legendre. 2002. Climatic and biological forcing of the vertical flux of biogenic particles under seasonal Arctic sea ice. *Marine Ecology Progress Series* **225**:1-16.
- Galley, R. J., D. Babb, M. Ogi, B. G. T. Else, N. X. Geilfus, O. Crabeck, D. G. Barber, and S. Rysgaard. 2016. Replacement of multiyear sea ice and changes in the open water season duration in the Beaufort Sea since 2004. *Journal of Geophysical Research: Oceans* **121**:1806-1823.
- Gosselin, M., M. Levasseur, P. A. Wheeler, R. A. Horner, and B. C. Booth. 1997. New measurements of phytoplankton and ice algal production in the Arctic Ocean. *Deep Sea Research Part II: Topical Studies in Oceanography* **44**:1623-1644.
- Gradinger, R. 2009. Sea-ice algae: Major contributors to primary production and algal biomass in the Chukchi and Beaufort Seas during May/June 2002. *Deep Sea Research Part II: Topical Studies in Oceanography* **56**:1201-1212.
- Gran, H. H. 1900. Diatomaceae from the ice-floes and plankton of the Arctic Ocean. Norwegian North Polar Expedition 1893-1896, Scientific Results **4**:1-74.
- Hansen, A. S., T. G. Nielsen, H. Levinsen, S. D. Madsen, T. F. Thingstad, and B. W. Hansen. 2003. Impact of changing ice cover on pelagic productivity and food web structure in Disko Bay, West Greenland: a dynamic model approach. *Deep Sea Research Part I: Oceanographic Research Papers* **50**:171-187.

- Hegseth, E. N., and A. Sundfjord. 2008. Intrusion and blooming of Atlantic phytoplankton species in the high Arctic. *Journal of Marine Systems* **74**:108-119.
- Holland, M. M., C. M. Bitz, and B. Tremblay. 2006. Future abrupt reductions in the summer Arctic sea ice. *Geophysical Research Letters* **33**.
- Horner, R., and G. Schrader. 1982. Relative contributions of ice algae, phytoplankton, and benthic microalgae to primary production in nearshore regions of the Beaufort Sea. *Arctic*:485-503.
- Hsiao, S. I. 1992. Dynamics of ice algae and phytoplankton in Frobisher Bay. *Polar Biology* **12**:645-651.
- IPCC. 2014. Climate change 2014: synthesis report. Contribution of Working Groups I, II and III to the fifth assessment report of the Intergovernmental Panel on Climate Change. 9291691437, IPCC, Geneva, Switzerland.
- Juul-Pedersen, T., C. Michel, and M. Gosselin. 2008a. Influence of the Mackenzie River plume on the sinking export of particulate material on the shelf. *Journal of Marine Systems* **74**:810-824.
- Juul-Pedersen, T., C. Michel, and M. Gosselin. 2010. Sinking export of particulate organic material from the euphotic zone in the eastern Beaufort Sea. *Marine Ecology Progress Series* **410**:55-70.
- Juul-Pedersen, T., C. Michel, M. Gosselin, and L. Seuthe. 2008. Seasonal changes in the sinking export of particulate material under first-year sea ice on the Mackenzie Shelf (western Canadian Arctic). *Marine Ecology Progress Series* **353**:13-25.
- Kahru, M., V. Brotas, M. Manzano-Sarabia, and B. Mitchell. 2011. Are phytoplankton blooms occurring earlier in the Arctic? *Global change in biology* **17**:1733-1739.
- Kohlbach, D., M. Graeve, B. A. Lange, C. David, I. Peeken, and H. Flores. 2016. The importance of ice algae-produced carbon in the central Arctic Ocean ecosystem: Food web relationships revealed by lipid and stable isotope analyses. *Limnology and Oceanography* **61**:2027-2044.
- Lalande, C., E. Bauerfeind, and E.-M. Nöthig. 2011. Downward particulate organic carbon export at high temporal resolution in the eastern Fram Strait: influence of Atlantic Water on flux composition. *Marine Ecology Progress Series* **440**:127-136.
- Lalande, C., E. M. Nöthig, and L. Fortier. 2019. Algal export in the Arctic Ocean in times of global warming. *Geophysical Research Letters*. doi.org/10.1029/2019GL083167
- Lavoie, D., K. L. Denman, and R. W. Macdonald. 2010. Effects of future climate change on primary productivity and export fluxes in the Beaufort Sea. *Journal of Geophysical Research: Oceans* **115**.
- LeBlanc, M., M. Geoffroy, C. Bouchard, S. Gauthier, A. Majewski, J. D. Reist, and L. Fortier. 2019. Pelagic production and the recruitment of juvenile polar cod *Boreogadus saida* in Canadian Arctic seas. *Polar Biology*:1-12.
- Leu, E., J. E. Søreide, D. O. Hessen, S. Falk-Petersen, and J. Berge. 2011. Consequences of changing sea-ice cover for primary and secondary producers in the European Arctic shelf seas: Timing, quantity, and quality. *Progress in Oceanography* **90**:18-32.
- Li, W. K. W., F. A. McLaughlin, C. Lovejoy, and E. C. Carmack. 2009. Smallest algae thrive as the Arctic Ocean freshens. *Science (New York, N.Y.)* **326**:539.
- Liu, J., J. A. Curry, Y. Dai, and R. Horton. 2007. Causes of the northern high-latitude land surface winter climate change. *Geophysical Research Letters* **34**.
- Liu, Y., and J. R. Key. 2014. Less winter cloud aids summer 2013 Arctic sea ice return from 2012 minimum. *Environmental Research Letters* **9**:044002.
- Michaud, J., L. Fortier, P. Rowe, and R. Ramseier. 1996. Feeding success and survivorship of Arctic cod larvae, *Boreogadus saida*, in the Northeast Water Polynya (Greenland Sea).

- Fisheries Oceanography **5**:120-135.
- Michel, C., L. Legendre, J.-C. Therriault, S. Demers, and T. Vandevelde. 1993. Springtime coupling between ice algal and phytoplankton assemblages in southeastern Hudson Bay, Canadian Arctic. *Polar Biology* **13**:441-449.
- Mundy, C., M. Gosselin, J. Ehn, Y. Gratton, A. Rossnagel, D. G. Barber, J. Martin, J. É. Tremblay, M. Palmer, and K. R. Arrigo. 2009. Contribution of under-ice primary production to an ice-edge upwelling phytoplankton bloom in the Canadian Beaufort Sea. *Geophysical Research Letters* **36**.
- Nicolaus, M., C. Katlein, J. Maslanik, and S. Hendricks. 2012. Changes in Arctic sea ice result in increasing light transmittance and absorption. *Geophysical Research Letters* **39**:501.
- Pauly, M. a. M., Tristan 2016. Arctic River Drainage Patterns. *In* C. C. I. Network, editor.
- Poulin, M., N. Daugbjerg, R. Gradinger, L. Ilyash, T. Ratkova, and C. von Quillfeldt. 2011. The pan-Arctic biodiversity of marine pelagic and sea-ice unicellular eukaryotes: a first-attempt assessment. *Marine Biodiversity* **41**:13-28.
- Reigstad, M., and P. Wassmann. 2007. Does *Phaeocystis* spp. contribute significantly to vertical export of organic carbon? *Biogeochemistry* **83**:217-234.
- Renaud, P. E., N. Morata, W. G. Ambrose Jr, J. J. Bowie, and A. Chiuchiolo. 2007. Carbon cycling by seafloor communities on the eastern Beaufort Sea shelf. *Journal of Experimental Marine Biology and Ecology* **349**:248-260.
- Sakshaug, E. 2004. Primary and secondary production in the Arctic Seas. Pages 57-81 *The organic carbon cycle in the Arctic Ocean*. Springer.
- Serreze, M. C., J. A. Maslanik, T. A. Scambos, F. Fetterer, J. Stroeve, K. Knowles, C. Fowler, S. Drobot, R. G. Barry, and T. M. Haran. 2003. A record minimum arctic sea ice extent and area in 2002. *Geophysical Research Letters* **30**.
- Serreze, M. C., and J. Stroeve. 2015. Arctic sea ice trends, variability and implications for seasonal ice forecasting. *Philosophical Transactions of the Royal Society A: Mathematical, Physical and Engineering Sciences* **373**:20140159.
- Simmonds, I., and K. Keay. 2009. Extraordinary September Arctic sea ice reductions and their relationships with storm behavior over 1979–2008. *Geophysical Research Letters* **36**.
- Søreide, J. E., E. Leu, J. Berge, M. Graeve, and S. Falk-Petersen. 2010. Timing of blooms, algal food quality and *Calanus glacialis* reproduction and growth in a changing Arctic. *Global change biology* **16**:3154-3163.
- Stabeno, P. J., N. A. Bond, N. B. Kachel, S. A. Salo, and J. D. Schumacher. 2001. On the temporal variability of the physical environment over the south-eastern Bering Sea. *Fisheries Oceanography* **10**:81-98.
- Stein, R., R. W. Macdonald, R. Stein, and R. W. MacDonald. 2004. The organic carbon cycle in the Arctic Ocean.
- Stern, G., and A. Gaden. 2015. From science to policy in the Western and Central Canadian Arctic: an Integrated Regional Impact Study (IRIS) of climate change and modernization. ArcticNet, Quebec Google Scholar.
- Stroeve, J., T. Markus, L. Boisvert, J. Miller, and A. Barrett. 2014. Changes in Arctic melt season and implications for sea ice loss. *Geophysical Research Letters* **41**:1216-1225.
- Stroeve, J. C., V. Kattsov, A. Barrett, M. Serreze, T. Pavlova, M. Holland, and W. N. Meier. 2012. Trends in Arctic sea ice extent from CMIP5, CMIP3 and observations. *Geophysical Research Letters* **39**.
- Syvertsen, E. E. 1991. Ice algae in the Barents Sea: types of assemblages, origin, fate and role in the ice-edge phytoplankton bloom. *Polar Research* **10**:277-288.
- Szymanski, A., and R. Gradinger. 2016. The diversity, abundance and fate of ice algae and phytoplankton in the Bering Sea. *Polar Biology* **39**:309-325.

- Tremblay, J.-É., and J. Gagnon. 2009. The effects of irradiance and nutrient supply on the productivity of Arctic waters: a perspective on climate change. Pages 73-93 Influence of climate change on the changing arctic and sub-arctic conditions. Springer.
- Tremblay, J.-É., K. Simpson, J. Martin, L. Miller, Y. Gratton, D. Barber, and N. M. Price. 2008. Vertical stability and the annual dynamics of nutrients and chlorophyll fluorescence in the coastal, southeast Beaufort Sea. *Journal of Geophysical Research: Oceans* **113**.
- Tremblay, J. É., S. Bélanger, D. Barber, M. Asplin, J. Martin, G. Darnis, L. Fortier, Y. Gratton, H. Link, and P. Archambault. 2011. Climate forcing multiplies biological productivity in the coastal Arctic Ocean. *Geophysical Research Letters* **38**.
- Turner, J. T. 2002. Zooplankton fecal pellets, marine snow and sinking phytoplankton blooms. *Aquatic microbial ecology* **27**:57-102.
- Utermöhl, H. 1958. Zur Vervollkommung der quantitativen phytoplankton-methodik. *Mitteilungen Internationale Verhandlungen Limnologie* **9**:38.
- Vancoppenolle, M., L. Bopp, G. Madec, J. Dunne, T. Ilyina, P. R. Halloran, and N. Steiner. 2013. Future Arctic Ocean primary productivity from CMIP5 simulations: Uncertain outcome, but consistent mechanisms. *Global Biogeochemical Cycles* **27**:605-619.
- Von Quillfeldt, C. 2000. Common diatom species in Arctic spring blooms: their distribution and abundance. *Botanica Marina* **43**:499-516.
- Von Quillfeldt, C. 2004. The diatom *Fragilariopsis cylindrus* and its potential as an indicator species for cold water rather than for sea ice. *Vie et milieu* **54**:137-144.
- Wang, M., and J. E. Overland. 2012. A sea ice free summer Arctic within 30 years: An update from CMIP5 models. *Geophysical Research Letters* **39**.
- Wassmann, P. 1997. Retention versus export food chains: processes controlling sinking loss from marine pelagic systems. *Hydrobiologia* **363**:29-57.
- Wassmann, P., and M. Reigstad. 2011. Future Arctic Ocean Seasonal Ice Zones and Implications for Pelagic-Benthic Coupling. *Oceanography* **24**:220-231.
- Welch, H. E., and M. A. Bergmann. 1989. Seasonal development of ice algae and its prediction from environmental factors near Resolute, NWT, Canada. *Canadian Journal of Fisheries and Aquatic Sciences* **46**:1793-1804.
- Werner, I., J. Ikävalko, and H. Schünemann. 2007. Sea-ice algae in Arctic pack ice during late winter. *Polar Biology* **30**:1493-1504.
- Williams, W. J., and E. C. Carmack. 2015. The 'interior' shelves of the Arctic Ocean: Physical oceanographic setting, climatology and effects of sea-ice retreat on cross-shelf exchange. *Progress in Oceanography* **139**:24-41.
- Wollenburg, J., C. Katlein, G. Nehrke, E.-M. Nöthig, J. Matthiessen, D. A. Wolf-Gladrow, A. Nikolopoulos, F. Gázquez-Sanchez, L. Rossmann, and P. Assmy. 2018. Ballasting by cryogenic gypsum enhances carbon export in a *Phaeocystis* under-ice bloom. *Scientific reports* **8**:7703.
- Yang, J. 2009. Seasonal and interannual variability of downwelling in the Beaufort Sea. *Journal of Geophysical Research: Oceans* **114**.